

## Report #1

1. However, I find it a little curious to see that one of the factors identified for this treatment is BBOA, which is known to vary within individual datasets (e.g. Young et al. (2015) Atmos. Chem. Phys., 15: 2429-2443, 10.5194/acp-15-2429-2015). It's also curious that they should select the optimum based on comparisons of the mass spectrum with previous studies. By doing this, I would see that what they are doing is little different to simply using the a priori reference spectrum in ME-2, thus defeating the whole purpose of the technique.

### **REPLY:**

Although BBOA varies across different datasets, the differences among different BBOAs are much less than those among different OA factors, which made BBOA identified by factorization in many studies. In this study, the purpose of comparing the BBOA anchor profiles from the unconstrained PMF results with the previous ones was just to confirm their basic BBOA characteristics, providing a new way to obtain a reasonable anchor profile for the ME-2 method, without the need to rely on a priori spectra. In the revised text, we have added the analysis that using the BBOA (and other POAs) spectra generated by the unconstrained PMF run of the same local dataset was indeed better than using a priori spectra from other studies, as in the reply to the next question.

2. Present a more robust theoretical case for the improvement in apportionment that could result from this method. While I would not ask the authors to submit a full mathematical proof, I would surmise that the factors that this would work best for this treatment would be the ones whose profiles are invariant (i.e. conform to the PMF data model) and produce a time series that is distinct from the other components. These should be explicitly stated and the implications of using factors that do not conform to these assumptions discussed. For instance, I would expect that if a factor has a profile that varies with time, one would expect that this would be under-represented in the unconstrained PMF solution (with some of its variability being represented by other factors) and therefore under-represented in the ME-2 solution.

### **REPLY:**

Both of the PMF and ME-2 methods assume that the source profiles are invariant with time during the whole campaigns, and the invariant source profiles identified by PMF or ME-2 are the relatively best selection to the final results in terms of statistics. In order to prove the improvement of using the anchor profiles generated by the unconstrained PMF run with the same local datasets, which do not depend on other studies, we also run the ME-2 analysis using the anchor profiles in the literature, with the results shown in Table 1-2. For Qingdao, the correlations between POAs and their tracers and the  $Q/Q_{\text{exp}}$  values using the three BBOA profiles in the literature are poorer than using the BBOA obtained in this study (Table 1). For Dongguan, the results from ME-2 using the HOA profiles in the literature are also poorer than using the HOA profiles obtained in this study (Table 2). Therefore, it can be seen that the method to get an anchor profile in this study is easier (it does not depend on the

literature) and more valid. We have added the above analysis in section 3 in the revised manuscript.

3. A step-by-step recommended procedure should be unambiguously presented, for the benefit of those attempting to recreate the method. While this is kind-of done in the conclusions, it is very vague in places.

**REPLY:**

We have adjusted the relevant text structures accordingly.

4. As a final technical query, can the authors confirm that the PAH data used to validate the result were not allowed to influence the factorisation originally? It would defeat the object of the exercise if they were.

**REPLY:**

The process of PAH quantification is now added in Section 2.4. The input matrix for PMF/ME-2 in this study does not include PAH fitting ions. We generally use the matrix with  $m/z$  of less than 100 (or 150) as the PMF/ME-2 input data, but the PAHs ions mostly have  $m/z$  of above 150. Therefore, the PAH data do not influence the factorization.

## References

- Crippa, M., DeCarlo, P. F., Slowik, J. G., Mohr, C., Heringa, M.F., Chirico, R., Poulain, L., Freutel, F., Sciare, J., Cozic, J., DiMarco, C. F., Elsasser, M., José, N., Marchand, N., Abidi, E., Wiedensohler, A., Drewnick, F., Schneider, J., Borrmann, S., Nemitz, E., Zimmermann, R., Jaffrezo, J.-L., Prévôt, A. S. H., and Baltensperger, U.: Wintertime aerosol chemical composition and source apportionment of the organic fraction in the metropolitan area of Paris, *Atmos. Chem. Phys.*, 13, 961–981, doi:10.5194/acp-13-961-2013, 2013.
- Crippa, M., Canonaco, V. a. Lanz, M. Äijälä, J. D. Allan, S. Carbone, G. Capes, D. Ceburnis, M. Dall'Osto, D. A. Day, P. F. DeCarlo, M. Ehn, a. Eriksson, E. Freney, L. Hildebrandt Ruiz, R. Hillamo, J. L. Jimenez, H. Junninen, A. Kiendler-Scharr, A. M. Kortelainen, M. Kulmala, A. Laaksonen, A. A. Mensah, C. Mohr, E. Nemitz, C. O'Dowd, J. Ovadnevaite, S. N. Pandis, T. Petäjä, L. Poulain, S. Saarikoski, K. Sellegri, E. Swietlicki, P. Tiitta, D. R. Worsnop, U. Baltensperger, and A. S. H. Prévôt: Organic aerosol components derived from 25 AMS data sets across Europe using a consistent ME-2 based source apportionment approach, *Atmos. Chem. Phys.*, 14(12), 6159-6176, doi: 10.5194/acp-14-6159-2014, 2014.

- Elser, M., R. J. Huang, R. Wolf, J. G. Slowik, Q. Wang, F. Canonaco, G. Li, C. Bozzetti, K. R. Daellenbach, Y. Huang, R. Zhang, Z. Li, J. Cao, U. Baltensperger, I. El-Haddad, and A. S. H. Prévôt : New insights into PM<sub>2.5</sub> chemical composition and sources in two major cities in China during extreme haze events using aerosol mass spectrometry, *Atmos. Chem. Phys.*, 16(5), 3207-3225, doi: 10.5194/acp-16-3207-2016,2016.
- He, L. Y., Y. Lin, X. F. Huang, S. Guo, L. Xue, Q. Su, M. Hu, S. J. Luan, and Y. H. Zhang : Characterization of high-resolution aerosol mass spectra of primary organic aerosol emissions from Chinese cooking and biomass burning, *Atmos. Chem. Phys.*, 10(23), 11535-11543, doi: 10.5194/acp-10-11535-2010,2010.
- Zheng J., Hu M., Gu F.T., Peng J.F., Zhang W.B., Xiao Y., Du Z.F., Qin Y.H., Deng L., Li M.R., Wu Y.S, Shuai S.J.: Characterization of High Resolution Source Profiles of Primary Organic Aerosol emissions From Gasoline Vehicles. *Proceedings of the CSEE.*, 36(16), 4466-4471,doi: 10.13334/j.0258-8013.pcsee.160358, 2016.

## Report #2

1. My general concern about the PMF technique on AMS OA spectra is that, is it reasonable to assume the number of factors and their profiles are always the same in different locations? Is it mathematically true that the more factors you allow PMF to resolve, the better the overall results would be? For example, in Line 133-135, the authors stated that BBOA and CCOA factors could be properly resolved by traditional PMF when the total number of factors was flexed up to 10. Also, the BBOA in Dongguan seems to be much more oxygenated than that in Qingdao, suggested by the much higher O/C ratio and OM/OC ratios. Could that be due to some factor mixing (i.e. BBOA mixed with OOA), or is it more reasonable to not assume they are both BBOA? E.g., maybe the Dongguan-BBOA should be characterized as aged BBOA or something similar? What are the reported ranges of O/C and OM/OC ratios for BBOA in literature?

### **REPLY:**

The numbers and types of factors were determined according to the unconstrained PMF results for each case, and could vary for different cases. For both the two sites in this paper, a 6-factor solution is chosen as the final result following the procedures detailed in Zhang et al. (2007). Crippa et al. (2014) also provides some guidelines to identify HOA, COA (check  $f_{55}/f_{57}$ ) and BBOA ( $f_{60}$ ) for ME-2, and the detailed information to identify the existence of CCOA is presented in our paper. Therefore,

we have enough evidence to expect four POA factors and two OOA factors for both sites in this study, and finally we got satisfactory running results. More OA factors output by ME-2 would not produce more significant factors. On the other hand, the purpose that we allow PMF to resolve more numbers is to find “purer” or more reasonable MS profiles (e.g., with a reasonable O/C ratio) for certain factors that were not well identified previously, not to look for a better overall result of PMF.

The range of O/C ratio and OM/OC ratio of BBOA reported in Canagaratna et al. (2015) is from 0.25 to 0.55, and from 1.50 to 1.88, respectively. But the fresh BBOA can be rapidly converted to OOA in less than 1 day (Bougiatioti et al., 2014), where the O/C ratio for aged BBOA could be up to 0.85 (Zheng et al., 2017). BBOA in Dongguan was apparently not fresh, considering it is an urban site and Dongguan has a warmer ambient air even in winter (17 °C in Dongguan; 9 °C in Qingdao), therefore the BBOA factor identified in Dongguan, with a strong contribution of m/z 60, has a higher O/C, indicating it is an aged and oxygenated BBOA. Following the suggestion of this reviewer, we will name this factor as Aged-BBOA in the revised paper.

2. Are there any industrial sources near the sampling sites at both cities? If so, please specify.

**REPLY:**

There is no industrial sources around the sampling sites, which has been clarified in the text.

3. Figure 3: I highly recommend the authors reorder the source profiles and time series plots in (a) and (b) so that they follow the same order for both sites for easier cross comparison.

**REPLY:**

We have corrected it.

4. Line 259: Please add some more details on how PAHs are derived from the OA spectra. You can also consider moving the details to Section 2.

**REPLY:**

We have added the details about the process of PAH quantification in Section 2.4.

5. Line 269: Are the ratios of PAHs to COA at the two sites in this study comparable to each other and other cities in the literature? Is there any compositional difference in the coals used for heating (and/or cooking) in the e.g. Northern and Southern China?

**REPLY:**

We didn't mention the ratios of PAHs to COA but the ratios of PAHs to OAs, and the ratio of PAHs to OAs (1.8%) in Qingdao was similar to that in the northern Chinese urban site of Xi'an (1.9%) (Elser et al., 2016) but was higher than that in Dongguan (0.9%) in Southern China. According to the spatial variation of heavy metal elements from coal (Tian et al., 2012), we can find that the emission compositions of coal combustion in different regions in China are quite similar. This information has been added into the revised text.

6. Line 275: correspond with -> are consistent with

**REPLY:**

We have corrected it.

7. Line 282: pollutants -> organic aerosol pollutants

**REPLY:**

We have corrected it.

**References**

- Bougiatioti, A., I. Stavroulas, E. Kostenidou, P. Zampas, C. Theodosi, G. Kouvarakis, F. Canonaco, A. S. H. Prévôt, A. Nenes, S. N. Pandis, and N. Mihalopoulos : Processing of biomass-burning aerosol in the eastern Mediterranean during summertime, *Atmos. Chem. Phys.*, 14(9), 4793-4807, doi: 10.5194/acp-14-4793-2014,2014.
- Canagaratna, M. R., J. L. Jimenez, J. H. Kroll, Q. Chen, S. H. Kessler, P. Massoli, L. Hildebrandt Ruiz, E. Fortner, L. R. Williams, K. R. Wilson, J. D. Surratt, N. M. Donahue, J. T. Jayne, and D. R. Worsnop : Elemental ratio measurements of organic compounds using aerosol mass spectrometry: characterization, improved calibration, and implications, *Atmos. Chem. Phys.*, 15(1), 253-272, doi: 10.5194/acp-15-253-2015,2015.
- Crippa, M., F. Canonaco, V. a. Lanz, M. Äijälä, J. D. Allan, S. Carbone, G. Capes, D. Ceburnis, M. Dall'Osto, D. A. Day, P. F. DeCarlo, M. Ehn, a. Eriksson, E. Freney, L. Hildebrandt Ruiz, R. Hillamo, J. L. Jimenez, H. Junninen, A. Kiendler-Scharr, A. M. Kortelainen, M. Kulmala, A. Laaksonen, A. A. Mensah, C. Mohr, E. Nemitz, C. O'Dowd, J. Ovadnevaite, S. N. Pandis, T. Petäjä, L. Poulain, S. Saarikoski, K. Sellegri, E. Swietlicki, P. Tiitta, D. R. Worsnop, U. Baltensperger, and A. S. H. Prévôt: Organic aerosol components derived from 25 AMS data sets across Europe using a consistent ME-2 based source apportionment approach, *Atmos. Chem. Phys.*, 14(12),6159-6176, doi: 10.5194/acp-14-6159-2014, 2014.
- Elser, M., R. J. Huang, R. Wolf, J. G. Slowik, Q. Wang, F. Canonaco, G. Li, C. Bozzetti, K. R. Daellenbach, Y. Huang, R. Zhang, Z. Li, J. Cao, U. Baltensperger, I. El-Haddad, and A. S. H. Prévôt : New insights into PM<sub>2.5</sub> chemical

composition and sources in two major cities in China during extreme haze events using aerosol mass spectrometry, *Atmos. Chem. Phys.*, 16(5), 3207-3225, doi: 10.5194/acp-16-3207-2016,2016.

Tian, H., Cheng, K., Wang, Y., Zhao, D., Lu, L., Jia, W. and Hao, J.: Temporal and spatial variation characteristics of atmospheric emissions of Cd, Cr, and Pb from coal in China. *Atmospheric Environment*, 50: 157-163,doi: 10.1016/j.atmosenv.2011.12.045,2012.

Zhang, Q., J. L. Jimenez, M. R. Canagaratna, J. D. Allan, H. Coe, I. Ulbrich, M. R. Alfarra, A. Takami, A. M. Middlebrook, Y. L. Sun, K. Dzepina, E. Dunlea, K. Docherty, P. F. DeCarlo, D. Salcedo, T. Onasch, J. T. Jayne, T. Miyoshi, A. Shimono, S. Hatakeyama, N. Takegawa, Y. Kondo, J. Schneider, F. Drewnick, S. Borrmann, S. Weimer, K. Demerjian, P. Williams, K. Bower, R. Bahreini, L. Cottrell, R. J. Griffin, J. Rautiainen, J. Y. Sun, Y. M. Zhang, and D. R. Worsnop :Ubiquity and dominance of oxygenated species in organic aerosols in anthropogenically-influenced Northern Hemisphere midlatitudes, *Geophys. Res. Lett.*, 34(13), L13801, doi: 10.1029/2007GL029979,2007.

Zheng, J., Hu, M., Du, Z., Shang, D., Gong, Z., Qin, Y., Fang, J., Gu, F., Li, M., Peng, J., Li, J., Zhang, Y., Huang, X., He, L., Wu, Y., and Guo, S.: Influence of biomass burning from South Asia at a high-altitude mountain receptor site in China, *Atmos. Chem. Phys.*, 17, 6853-6864, <https://doi.org/10.5194/acp-17-6853-2017>, 2017.

## List of all relevant changes

Line 64:

...and there is no industrial emission nearby.

Line 108:

### 2.4 Polycyclic aromatic hydrocarbons (PAHs) quantification

In this study, PAHs mass concentrations were quantitatively determined from the HR-AMS data. The steps outlined are as follows: first, the PAHs molecular ions  $[M]^+$ , including  $[C_{10}H_8]^+$ ,  $[C_{12}H_8]^+$ ,  $[C_{14}H_8]^+$ ,  $[C_{14}H_{10}]^+$ ,  $[C_{16}H_{10}]^+$ ,  $[C_{18}H_{10}]^+$ ,  $[C_{18}H_{12}]^+$ ,  $[C_{20}H_{12}]^+$ ,  $[C_{22}H_{12}]^+$ ,  $[C_{22}H_{14}]^+$ ,  $[C_{24}H_{12}]^+$ ,  $[C_{24}H_{14}]^+$ , and other associated fragments, including  $[M-H]^+$ ,  $[M-2H]^+$ ,  $[M]^{2+}$ , and  $[M-H]^{2+}$  were fitted in the HR spectra. Second, the fragments presented low correlation (i.e.,  $R^2$  below 0.6) with their corresponding molecular ions were not taken into account. Finally, the relative ionization efficiency (RIE) for PAHs was assumed to be 1.4 and the dependency of the collection efficiency ( $CE_b$ ) on the chemical composition of the aerosol was estimated using a composition-dependent collection efficiency (CDCE) algorithm (Middlebrook et al., 2012). More details about the method can be found in Bruns et al. (2015).

Line 145:

...the BBOA anchor profile should be investigated, and we attempted to look for it from the unconstrained PMF results based on the same dataset, and found that the BBOA factors in the 7- and 8-factor solutions might be used as the anchor profiles. They both had good correlation with the BBOA MS in Chinese biomass burning emission simulation (He et al., 2010), confirming their basic BBOA characteristics.

Line 160:

Tian et al. (2012) also found that the emission compositions of coal combustion in different regions in China are quite similar.

Line 193:

In order to prove the improvement of using the anchor profiles generated by the unconstrained PMF run with the same local datasets, we also run the ME-2 analysis using the anchor profiles available in the literature, with the results shown in Table S5 and S6. For Qingdao, the correlations between POAs and their tracers and the Q/Qexp values using the three BBOA profiles in the literature are poorer than using the BBOA obtained in this study (Table S5). For Dongguan, the results from ME-2 using the HOA profiles in the literature are also poorer than using the HOA profiles obtained in this study (Table S6). Therefore, it can be clearly seen that the method to obtain an anchor profile in this study is easier (it does not depend on the results in the literature) and

more valid.

Line 242:

Although the range of the O/C ratio of BBOA reported in Canagaratna et al. (2015) was from 0.25 to 0.55, fresh BBOA was found to be rapidly converted to OOA in less than 1 day (Bougiatioti et al., 2014), and the O/C ratio of aged BBOA could be up to 0.85 (Zheng et al., 2017). BBOA in Dongguan was apparently not fresh considering it is an urban site and Dongguan has a warmer winter (17 °C in Dongguan vs. 9 °C in Qingdao). The BBOA factor identified in Dongguan, with a strong contribution of m/z 60, had a higher O/C, indicating it was an oxygenated BBOA, therefore we name it Aged-BBOA in this study.



# Improved source apportionment of organic aerosols in complex urban air pollution using the multilinear engine (ME-2)

Qiao Zhu<sup>1</sup>, Xiao-Feng Huang<sup>1,\*</sup>, Li-Ming Cao<sup>1</sup>, Lin-Tong Wei<sup>1</sup>, Bin Zhang<sup>1</sup>, Ling-Yan He<sup>1</sup>, Miriam Elser<sup>2</sup>, Francesco Canonaco<sup>2</sup>, Jay G. Slowik<sup>2</sup>, Carlo Bozzetti<sup>2</sup>, Imad El-Haddad<sup>2</sup>, and André S.H. Prévôt<sup>2</sup>

<sup>1</sup>Key Laboratory for Urban Habitat Environmental Science and Technology, School of Environment and Energy, Peking University Shenzhen Graduate School, Shenzhen, 518055, China.

<sup>2</sup>Paul Scherrer Institute (PSI), 5232 Villigen-PSI, Switzerland

**Abstract** Organic aerosols (OAs), which consist of thousands of complex compounds emitted from various sources, constitute one of the major components of fine particulate matter. The traditional positive matrix factorization (PMF) method often apportions aerosol mass spectrometer (AMS) organic datasets into less meaningful or mixed factors, especially in complex urban cases. In this study, an improved source apportionment method using a bilinear model of the multilinear engine (ME-2) was applied to OAs collected during the heavily polluted season from two Chinese megacities located in the north and south with an Aerodyne high-resolution aerosol mass spectrometer (HR-ToF-AMS). We applied a rather novel procedure for utilization of prior information and selecting optimal solutions, which does not necessarily depend on other studies. Ultimately, six reasonable factors were clearly resolved and quantified for both sites by constraining one or more factors: hydrocarbon-like OA (HOA), cooking-related OA (COA), biomass burning OA (BBOA), coal combustion (CCOA), less-oxidized oxygenated OA (LO-OOA) and more-oxidized oxygenated OA (MO-OOA). In comparison, the traditional PMF method could not effectively resolve the appropriate factors, e.g., BBOA and CCOA, in the solutions. Moreover, coal combustion and traffic emissions were determined to be primarily responsible for the concentrations of PAHs and BC, respectively, through the regression analyses of the ME-2 results.

## 1 Introduction

Atmospheric aerosols are generating increasing interest due to their adverse effects on human health, visibility and the climate (IPCC, 2013; Pope and Dockery, 2006). Among different particulate compositions, many studies focus on organic aerosols (OAs) because they contribute 20-90% to the total submicron mass (Jimenez et al., 2009; Zhang et al., 2007). OAs can be either directly emitted by various sources, including anthropogenic (i.e., traffic and combustion activities) and biogenic sources, or produced via secondary formation after the oxidation of volatile organic compounds (VOCs) (Hallquist et al., 2009).

---

<sup>1</sup> Correspondence to: X.-F. Huang (huangxf@pku.edu.cn)

27 Therefore, the reliable source identification and quantification of OAs are essential before developing effective political  
28 abatement strategies.

29 Aerodyne aerosol mass spectrometer (AMS) systems are the most widely adopted on-line aerosol measurement systems  
30 for acquiring aerosol chemical compositions (Canagaratna et al., 2007; Pratt and Prather, 2012). An AMS provides on-line  
31 quantitative mass spectra of non-refractory components from the submicron aerosol fraction with a high temporal resolution  
32 (i.e., seconds to minutes) (Canagaratna et al., 2007). The total mass spectra can be assigned to both several inorganic  
33 compounds and the organic fraction through mass spectral fragmentation tables (Allan et al., 2004). To further investigate the  
34 different types of organic fractions, numerous studies have exploited the positive matrix factorization (PMF) algorithm and  
35 apportioned the AMS organic mass spectra in terms of their source emissions or formation processes (Zhang et al., 2011).  
36 PMF is a standard multivariate factor analysis tool (Paatero, 1999; Paatero and Tapper, 1994) that models the time series of  
37 measured organic mass spectra as a linear combination of positive factor profiles and their respective time series. Most of the  
38 earlier PMF studies were conducted on unit-mass resolution (UMR) mass spectrometers (Lanz et al., 2007; Lanz et al., 2010;  
39 Ulbrich et al., 2009), although more have recently focused on high-resolution (HR) mass spectra PMF (Aiken et al., 2009;  
40 Docherty et al., 2008; Huang et al., 2010). The use of HR mass spectra data to constrain PMF solutions can reduce their  
41 rotational ambiguity and result in more interpretable OA factors. For example, Aiken et al. (2009) found that hydrocarbon-like  
42 OA (HOA) and biomass burning OA (BBOA) were better separated using HR-AMS data than with UMR data. However, even  
43 HR-AMS-PMF can also yield mixed factors (especially in heavily polluted areas) due to their complex emission patterns.

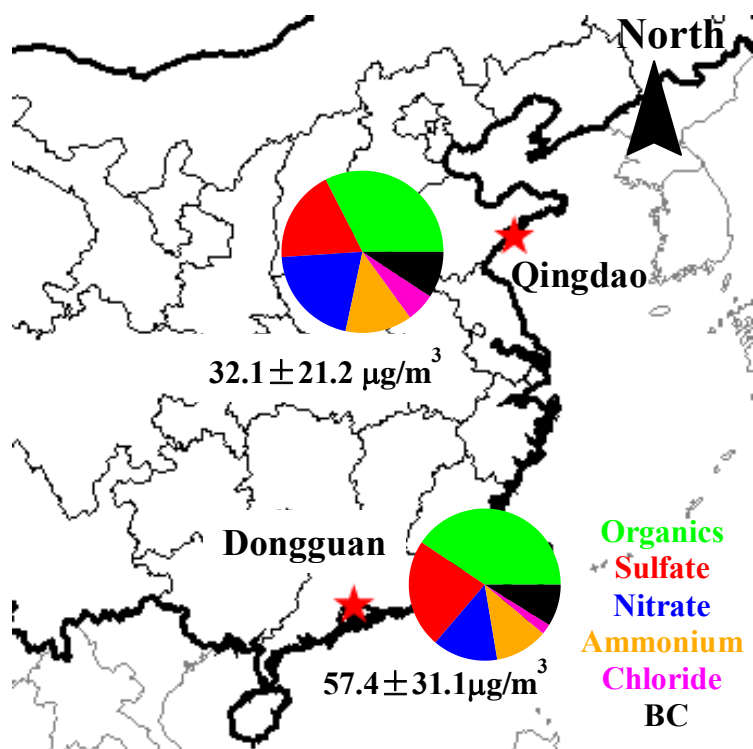
44 The abundant characteristic fragments for cooking-related OA (COA) (e.g.,  $m/z$  55 and 57) and coal combustion OA  
45 (CCOA) (e.g.,  $m/z$  51, 53, and 65) can be observed in the mass spectrum of the HOA factor (He et al., 2010; Hu et al., 2013).  
46 Elser (et al., 2016) analyzed two urban HR-AMS datasets in China, and their PMF results showed an HOA profile that  
47 contained a high concentration of  $C_2H_4O_2^+$  ( $m/z$  60), which is a BBOA tracer ion. In addition,  $CO_2^+$  ( $m/z$  44) contributed more  
48 to COA compared to oxygenated OA (OOA). To solve this “mixed factor” problem in PMF analysis, some researchers  
49 attempted to use the multilinear engine algorithm (ME-2) with user-provided constraints (Canonaco et al., 2013; Crippa et al.,  
50 2014; Elser et al., 2016; Reyes-Villegas et al., 2016). However, several key issues with the ME-2 in these studies, such as  
51 reliability of the user-input constraints and the criteria used to determine an optimal result, still require further investigation.  
52 Most ME-2 studies (Crippa et al., 2014; Elser et al., 2016; Reyes-Villegas et al., 2016) were based on HR-AMS datasets and  
53 utilized mass profiles of PMF results from Paris (Crippa et al., 2013; mostly due to the lack of other reliable source profiles)  
54 and did not consider the specific sampling sites, which could result in uncertainties.

55 In this study, a novel source apportionment technique using the multi-linear engine tool (ME-2) was successfully applied  
56 to organic mass spectra obtained with an HR-ToF-AMS at two urban sites during pollution-heavy periods during the same  
57 year. The improved OA source apportionment results are discussed and compared with an unconstrained PMF analysis.

## 58 2 Materials and methods

### 59 2.1 Sampling sites and period

60 Measurements at Qingdao (36.10°N, 120.47°E, 10 m above ground level, a.g.l.) were performed from 1 to 31 November  
61 2013, while those in Dongguan were conducted from 12 December 2013 to 1 January 2014 (33.03°N, 113.75°E, 100 m a.g.l.).  
62 Qingdao is a coastal city with over 9 million inhabitants in northern China, while Dongguan has over 8 million inhabitants and  
63 is located in southern China (shown in Figure 1). Both of the sampling sites are on the tops of buildings in urban central areas,  
64 and there is no industrial emission nearby.  
65



66  
67 **Figure 1.** The locations and the average PM<sub>1</sub> chemical compositions of the Qingdao and Dongguan sampling sites.

### 68 2.2 Instrumentation

69 An HR-ToF-AMS was deployed for the on-line measurement of non-refractory PM<sub>1</sub> (Canagaratna et al., 2007). The setup  
70 and operation of the HR-ToF-AMS was similar to that in our previous studies (Huang et al., 2015; Huang et al., 2010). A PM<sub>2.5</sub>  
71 cyclone inlet was briefly placed on the roof of a building to remove coarse particles and to introduce an air stream containing  
72 the remaining particles into a room through a copper tube with a flow rate of 10 l min<sup>-1</sup>. A nafion dryer (MD-070-12S-4, Perma  
73 Pure Inc.) was positioned upstream of the HR-ToF-AMS to eliminate the potential influence of relative humidity on the

74 particle collection (Matthew et al., 2008), after which the HR–ToF–AMS isokinetically sampled from the center of the copper  
75 tube at a flow rate of 80 ml min<sup>-1</sup>. The instrument was operated at two ion optical modes with a cycle of 4 min, including 2  
76 min for the mass-sensitive V-mode and 2 min for the high mass resolution W-mode. An aethalometer (AE-31, Magee), which  
77 also has a PM<sub>2.5</sub> inlet, was simultaneously used for measurements of refractory black carbon (BC) with a temporal resolution  
78 of 5 min.

79 A routine analysis of the HR–ToF–AMS data was performed using the software SQUIRREL (version 1.57) and PIKA  
80 (version 1.16) written in Igor Pro 6.37 (Wave Metrics  
81 Inc.)(<http://cires1.colorado.edu/jimenezgroup/ToFAMSResources/ToFSoftware/index.html>). The ionization efficiency (IE)  
82 was calibrated using pure ammonium nitrate particles following standard protocols (Drewnick et al., 2005; Jayne et al.,  
83 2000). The relative IEs (RIEs) for organics, nitrate and chloride were assumed to be 1.4, 1.1 and 1.3, respectively. A  
84 composition-dependent collection efficiency (CE) was applied to the data based on the method of Middlebrook et al. (2012)  
85 and an organic elemental analysis was performed using the latest approach recommended by Canagaratna et al. (2015).

### 86 **2.3 PMF and ME-2 methods for OA source apportionment**

87 PMF is a mathematical technique used to solve bilinear unmixing problems (Paatero and Tapper, 1994) that enables a  
88 description of the variability of a multivariate database as the linear combination of static factor profiles and their  
89 corresponding time series. The bilinear factor analytic model in matrix notation is defined in Eq. (1), where the measured  
90 matrix X (consisting of i rows and j columns) is approximated by the product of G (containing the factor time series) and F  
91 (the factor profiles). E denotes the model residuals. The entries in G and F are fitted using a least-squares algorithm that  
92 iteratively minimizes the quantity Q (Eq. 2), which is defined as the sum of the squared residuals ( $e_{ij}$ ) weighted by their  
93 respective uncertainties ( $\sigma_{ij}$ ).

$$94 \quad X = G \times F + E \quad (1)$$

$$95 \quad Q = \sum_{i=1}^m \sum_{j=1}^n \left( \frac{e_{ij}}{\sigma_{ij}} \right)^2 \quad (2)$$

96 In this study, we adopted SoFi (Canonaco et al., 2013), which is an implementation of the multilinear engine (ME-2)  
97 (Paatero, 1999), to perform the organic HR-AMS data analysis. In contrast to an unconstrained PMF analysis, ME-2 enables  
98 a more complete exploration of the rotational ambiguity of the solution space. In our case, this is achieved by directing the  
99 solution towards environmentally meaningful rotations using the *a* value approach. This method uses prior input profiles and  
100 the scalar *a* to constrain one or more output factor profiles such that they fall within a predetermined range. The *a* value  
101 determines the extent to which the output profiles are allowed to vary from the input profiles according to Eq. (3), where *f*  
102 represents the factor profile and *j* indicates the *m/z* of the ions.

$$103 \quad f_{j,\text{solution}} = f_j \pm a \times f_j \quad (3)$$

104 The number of output factors, which is selected by the user, is a key consideration for PMF analysis. Most unconstrained PMF  
105 results were chosen following the procedures detailed in Zhang et al. (2007). However, additional outputs in ME-2 can be

106 generated to explore more of the solution space, and more criteria should be developed to support the factor identification,  
107 which will be discussed in section 3.

## 108 **2.4 Polycyclic aromatic hydrocarbons (PAHs) quantification**

109 In this study, PAHs mass concentrations were quantitatively determined from the HR-AMS data. The steps outlined are  
110 as follows: first, the PAHs molecular ions  $[M]^+$ , including  $[C_{10}H_8]^+$ ,  $[C_{12}H_8]^+$ ,  $[C_{14}H_8]^+$ ,  $[C_{14}H_{10}]^+$ ,  $[C_{16}H_{10}]^+$ ,  $[C_{18}H_{10}]^+$ ,  
111  $[C_{18}H_{12}]^+$ ,  $[C_{20}H_{12}]^+$ ,  $[C_{22}H_{12}]^+$ ,  $[C_{22}H_{14}]^+$ ,  $[C_{24}H_{12}]^+$ ,  $[C_{24}H_{14}]^+$ , and other associated fragments, including  $[M-H]^+$ ,  $[M-2H]^+$ ,  
112  $[M]^{2+}$ , and  $[M-H]^{2+}$  were fitted in the HR spectra. Second, the fragments presented low correlation (i.e.,  $R^2$  below 0.6) with  
113 their corresponding molecular ions were not taken into account. Finally, the relative ionization efficiency (RIE) for PAHs was  
114 assumed to be 1.4 and the dependency of the collection efficiency ( $CE_b$ ) on the chemical composition of the aerosol was  
115 estimated using a composition-dependent collection efficiency (CDCE) algorithm (Middlebrook et al., 2012). More details  
116 about the method can be found in Bruns et al. (2015).

## 117 **3 Interpretation of OA source apportionment using ME-2**

118 In this section, a conventional PMF without any prior information is performed to analyze the OA source apportionment.  
119 Then, we use the ME-2 method to optimize the OA source apportionment based on the information obtained from the PMF  
120 method. The sequential steps are reported below:

### 121 1. Unconstrained PMF runs.

122 We performed unconstrained runs with a range from two to ten factors. Generally, PMF solutions with large numbers of  
123 factors are not considered due to possible mathematical splits of the factor profiles. However, some factors that have small  
124 contributions or that have similar mass profiles as other factors (but different time series) may only be found in solutions with  
125 large numbers of factors. We observe that most of the solutions provided via PMF include either multiply split factors or mixed  
126 factors that are not properly separated from one another. In other words, PMF does not produce an appropriate solution. The  
127 6-factor solutions for Qingdao and Dongguan are shown in Figure S1 and S2, and three types of primary OAs (POAs) were  
128 identified for each sampling site, including HOA), coal combustion OA (CCOA) and cooking OA (COA) for Qingdao and  
129 HOA, biomass burning OA (BBOA) and COA for Dongguan. Oxygenated OA (OOA) seems to be excessively split in the 6-  
130 factor solutions for both of the sites. HOA is distinguished by alkyl fragment signatures with prominent contributions of  $m/z$   
131 55 ( $C_4H_7^+$ ) and  $m/z$  57 ( $C_4H_9^+$ ) (Ng et al., 2011). The COA profile is similar to that of HOA but has a higher contribution from  
132 oxygenated ions at  $m/z$  55 ( $C_3H_3O^+$ ) and  $m/z$  57 ( $C_3H_5O^+$ ) (Mohr et al., 2012). BBOA is characterized by the presence of  
133 signals at  $m/z$  60 ( $C_2H_4O_2^+$ ) and  $m/z$  73 ( $C_3H_5O_2^+$ ), which are identified as fragments from anhydrous sugars present in biomass  
134 smoke (Alfarra et al., 2007). The OOA profile is characterized by a high signal at  $m/z$  44 ( $CO_2^+$ ). Note that some POA profiles  
135 in this solution indicate mixing; for example, CCOAs in Qingdao contain a high concentration of the biomass burning tracer  
136 ion ( $m/z$  60,  $C_2H_4O_2^+$ ), and HOAs in Dongguan have a higher-than-expected contribution of  $m/z$  44 ( $CO_2^+$ ) with a high O/C

137 ratio (0.26). In addition, CCOA seems to be mixed with BBOA. We then further verified the solutions with additional factors.  
138 The results show that BBOA and CCOA are separated from each other in the 7- and 8-factor solutions for Qingdao (see Figure  
139 S1) and that better signals for unmixed and stable HOA with low O/C ratios of 0.17 or 0.18 emerged in the 7- to 10-factor  
140 solutions for Dongguan (see Figure S2).

## 141 2. Investigate anchor profiles for ME-2.

142 Before operating ME-2, feasible and reasonable prior input profiles must be determined. To the best of our knowledge,  
143 this is the first HR-OA data set that employs anchor profiles extracted from an unconstrained PMF solution with a higher  
144 number of factors, and the same approach has been successfully applied to source apportionment efforts using UMR ME-2  
145 (Fröhlich et al., 2015). In our case for Qingdao, the BBOA anchor profile should be investigated, and we attempted to look for  
146 it from the unconstrained PMF results based on the same dataset, and found that the BBOA factors in the 7- and 8-factor  
147 solutions might be used as the anchor profiles. They both had good correlation with the BBOA MS in Chinese biomass burning  
148 emission simulation (He et al., 2010), confirming their basic BBOA characteristics. Although these two BBOA factors are  
149 quite similar, the BBOA from the 8-factor solution is better suited to be a constraining profile due to its smaller  $m/z$  44 ( $\text{CO}_2^+$ )  
150 signal and higher  $m/z$  60 ( $\text{C}_2\text{H}_4\text{O}_2^+$ ) signal (see Figure S3). In addition, the BBOA from the 8-factor solution also correlates  
151 better with the BBOA from a Chinese biomass burning simulation ( $R^2=0.81$ ) than the 7-factor solution ( $R^2=0.79$ ). For  
152 Dongguan, the anchor profile for HOA can be obtained from unconstrained PMF solutions. The averaged HOA profile from  
153 the 7- to 10-factor solutions was used as the anchor profile for ME-2 due to the small differences among the different solutions.  
154 Additionally, the constraining CCOA profile for Dongguan is still under consideration because the mass spectrum of BBOA  
155 was found to be very similar to that of CCOA, raising the concern that coal combustion particles might have been incorrectly  
156 apportioned to biomass burning sources (Wang et al., 2013). An appropriate CCOA anchor profile could not be obtained due  
157 to an increase in the unconstrained PMF factor number (see Figure S2). The best approach is to employ the CCOA profile  
158 from Qingdao as the constraining profile for Dongguan in ME-2, as these two campaigns were conducted using the same HR-  
159 ToF-AMS in the same year. In addition, the CCOA from Qingdao has a very good correlation ( $R^2=0.97$ ) with CCOA profiles  
160 reported at other Chinese urban sites (Elser et al., 2016) (see Figure S4). Tian et al. (2012) also found that the emission  
161 compositions of coal combustion in different regions in China are quite similar. The input profiles for BBOA, HOA and CCOA  
162 prior to operating ME-2 are shown in Figure 2.

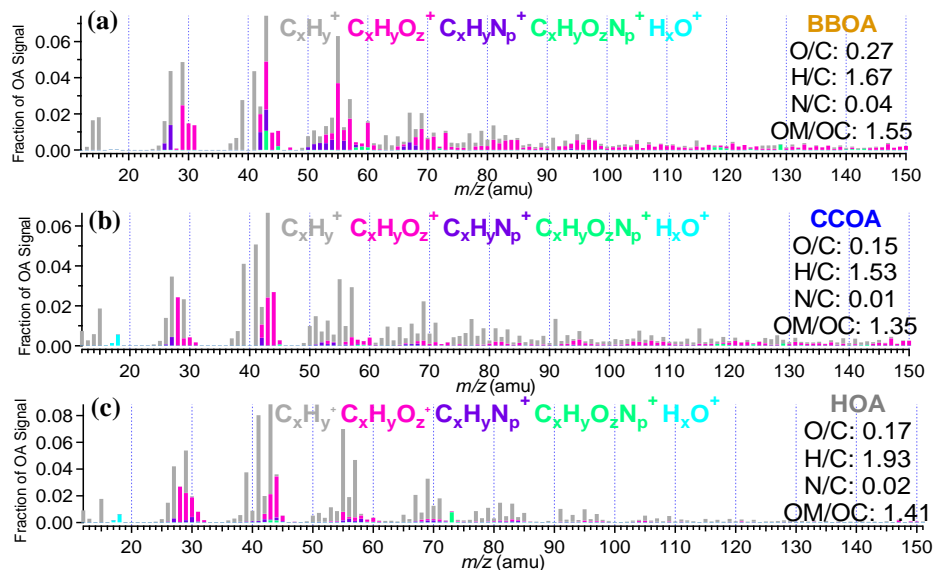


**Figure 2.** The anchor mass spectra for (a) BBOA, (b) CCOA and (c) HOA in the ME-2 analysis.

3. Constrain the mass spectrums of the mixed factors with different  $a$  values.

According to the unconstrained PMF results, the best interpretable results for both two sites are the 6-factor solutions with factors that include HOA, COA, BBOA, CCOA, less-oxidized oxygenated OA (LO-OOA) and more-oxidized oxygenated OA (MO-OOA) (Figure 3a and 3b). The  $a$  values set from 0 to 1 with an increment of 0.1 for BBOA in Qingdao yields 11 possible solutions, and for both HOA and CCOA in Dongguan yields 121 possible solutions.

4. Criteria for obtaining the optimal results.

In this study, we used two simple and reasonable criteria to obtain a better environmental OA source apportionment: the reasonability of the O/C ratio and the correlation between the factors and the tracers. For Qingdao, the O/C ratios for six resolved factors and the correlations between CCOA and PAHs, HOA and BC for 11 solutions with different  $a$  values are shown in Table S2. These results indicate that all of the O/C ratios for each factor and each factor-tracer correlation are quite similar to one another and that they agree with the range of values in the literature (Canagaratna et al., 2015). Therefore, the solutions averaged over the 11 outputs were considered the final results for Qingdao. For Dongguan, all of the O/C ratios for HOA, CCOA, COA and BBOA among the 121 possible solutions are listed in Table S3. The O/C ratio of HOA in the unconstrained PMF results remained between approximately 0.17 and 0.18, providing a filter criterion with which to assess reasonable ME-2 solutions, and only solutions with  $a$  values between 0 and 0.1 fell into this range (Table S1). The O/C ratios of other factors for  $a$  values between 0 and 0.1 are shown in Table S3. The solutions using  $a$  values between 0 and 0.1 for the HOA profile and an  $a$  value of 0.9 for the CCOA profile are considered ideal results for three reasons. First, unlike the HOA mass spectra, CCOAs from different sites show higher variability and the CCOA anchor profile is not derived from itself, and therefore, it is reasonable to restrict the constraint with small  $a$  values for HOA and a looser constraint should be applied for CCOA, which is consistent with the  $a$  values selecting rules in London ME-2 study (Reyes-Villegas et al., 2016). Second, the

186 POA factors in Dongguan, including HOA and CCOA, have higher O/C ratios likely as a result of a higher atmospheric  
187 oxidizing capacity and a stronger photochemical formation in Southern China (Hofzumahaus et al., 2009). Moreover, some  
188 studies reported that BBOAs undergo substantial chemical processing immediately after emission and that aged BBOAs had  
189 significant concentrations in fresh plumes (Zhou et al., 2017). Thus, CCOAs in Dongguan are very likely to demonstrate  
190 relatively higher ages than those in Qingdao (0.15) with higher O/C ratios (but with an O/C ratio of up to 1.25 when the  $a$   
191 value is 1, which is unacceptable). Third, with an increase in the  $a$  value for CCOA, two types of OOAs become more  
192 distinctive, and the factor correlates better with the tracer (Table S1 and Table S4).

193 In order to prove the improvement of using the anchor profiles generated by the unconstrained PMF run with the same  
194 local datasets, we also run the ME-2 analysis using the anchor profiles available in the literature, with the results shown in  
195 Table S5 and S6. For Qingdao, the correlations between POAs and their tracers and the  $Q/Q_{exp}$  values using the three BBOA  
196 profiles in the literature are poorer than using the BBOA obtained in this study (Table S5). For Dongguan, the results from  
197 ME-2 using the HOA profiles in the literature are also poorer than using the HOA profiles obtained in this study (Table S6).  
198 Therefore, it can be clearly seen that the method to obtain an anchor profile in this study is easier (it does not depend on the  
199 results in the literature) and more valid.

## 200 4 Results and discussion

### 201 202 4.1 Variations in the OA factors

203 Figure 1 shows the chemical compounds of  $PM_{10}$ , including the non-refractory (NR) components measured via HR-AMS  
204 (i.e., OA,  $SO_4$ ,  $NO_3$ ,  $NH_4$  and Cl) and BC concentrations measured via the AE-31, during the sampling period in both Qingdao  
205 and Dongguan. The average  $PM_{10}$  mass concentration was  $32.1 \pm 21.2 \mu g/m^3$  (mean  $\pm$  standard deviation) in Qingdao and  
206  $57.4 \pm 31.1 \mu g/m^3$  in Dongguan. The temporal variations in the  $PM_{10}$  species in conjunction with meteorological parameters are  
207 shown in Figure S5. Although Dongguan is located in southern China with relatively less air pollution (Huang et al., 2012),  
208 the  $PM_{10}$  mass concentration was higher. This is mainly because of stagnant meteorological conditions with low average wind  
209 speeds (i.e., 2.3 m/s) and a maximum wind speed of less than 6 m/s. Among the  $PM_{10}$  compounds, OAs accounted for 32.5%  
210 of  $PM_{10}$  in Qingdao and 40.6% in Dongguan. This suggests that OA constitutes a very important fraction at both urban sites.  
211 Thus, the final and detailed results of the OA source apportionment are presented in this section.

212 For Qingdao, the final result is the average of all of the ME-2 runs with constraints including  $a$  values from 0 to 1 fulfilling  
213 the criteria described in section 3.2. The mass spectra and time series of the resolved OA sources are shown in Figure 3a. The  
214 characteristics of each factor were distinct. The BBOA profile contained the highest  $m/z$  60 fraction  $f_{60}$  (1.5%) compared to  
215 the other factors, and the concentrations were highly correlated with  $C_2H_4O_2^+$  ( $R^2=0.81$ ). The mass spectra of COA was  
216 characterized by a high  $m/z$  55/57 ratio, which is consistent with previous results (He et al., 2010; Mohr et al., 2012; Sun et al.,

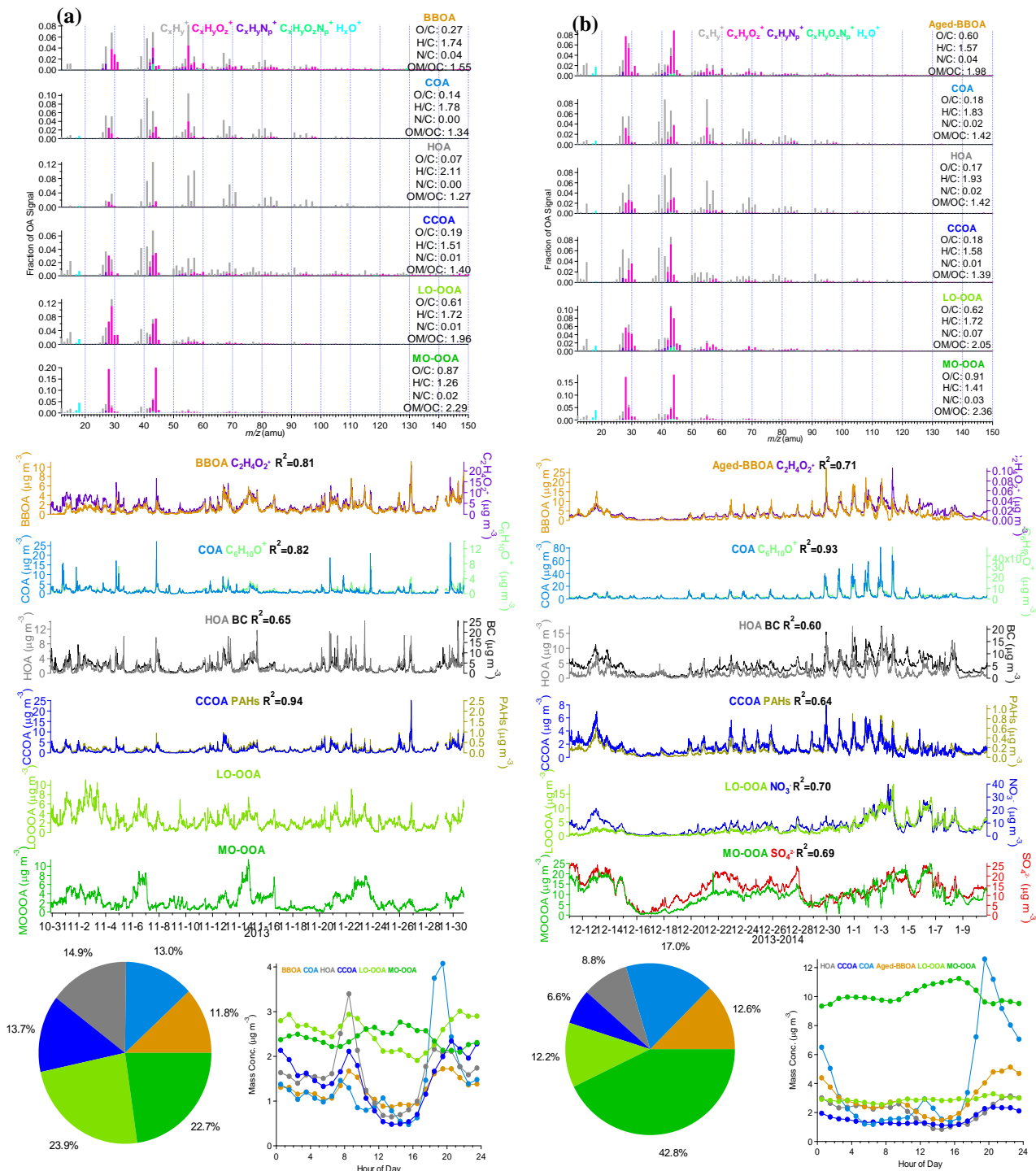


217 2016). In addition, the time series of COA showed a good correlation with its tracer ion  $C_6H_{10}O^+$  in accordance with (Sun et  
218 al., 2016). HOAs were correlated well with BC ( $R^2=0.65$ ), and CCOAs were highly correlated with PAHs ( $R^2=0.94$ ). Among  
219 the two types of OOAs, the less-oxidized OOA (LO-OOA) had a lower  $CO_2^+$  fraction and O/C ratio (0.62) compared with the  
220 more oxidized OOA (MO-OOA), which had a higher  $CO_2^+$  fraction and O/C (0.91) ratio. The sum of LO-OOA and MO-OOA  
221 showed a high correlation with the sum of sulfate and nitrate ( $R^2=0.76$ ). The POAs (including HOA, COA, BBOA and CCOA)  
222 contributed 53.4% to the OA concentration (Figure 3a), which was almost equal to the SOA fraction. In terms of the diurnal  
223 trends of the OA factors shown in Figure 3a, they are all partially driven both by PBL dynamics (demonstrating an increased  
224 dilution during the daytime and an accumulation of particulate matter overnight) and by the diurnal emission profile. The  
225 diurnal trend of HOA showed pronounced peaks during the morning and evening rush hours (8:00-9:00 and 19:00-21:00),  
226 which is typically the case for traffic-related pollutants. COA shows a very distinct daily trend with strong peaks during the  
227 lunch (approximately 12:00) and dinner (19:00-20:00) periods. CCOAs constituted an important and dominant source of  
228 pollutants during the wintertime in northern Chinese areas (Elser et al., 2016) due to heating activities, especially with regard  
229 to the central-heating supply that began on November 13 and continued until the end of the campaign. The diurnal variations  
230 of the four POA factors before and during the central-heating period are shown in Figure S6. In comparison with the other  
231 three POAs, the diurnal pattern of CCOA showed a clear increase during the central-heating period with concentration peaks  
232 during the morning (at approximately 9:00) and at night (starting to rise at 18:00), which seems consistent with heating  
233 emissions and atmospheric dilution. The diurnal trends of BBOA were similar to those of CCOA. The dilution of these particles  
234 within a deeper PBL during the daytime resulted in a decreasing trend in the BBOA concentration, while peaks related to  
235 residential heating were observed during the morning (between 09:00 to 10:00) and at night (starting to rise at 17:00). The  
236 main difference between the LO-OOA and MO-OOA diurnal patterns is that an increase in the MO-OOA mass concentration  
237 was observed during the daytime, implying that the formation of secondary organic aerosols was greatly enhanced during the  
238 afternoon. In addition, the diurnal cycle for LO-OOA showed a relatively smaller decrease during the daytime compared with  
239 the POA factors. These characteristics of the OOA diurnal trend confirm their secondary nature.

240 For Dongguan, similar to the OA source apportionment using ME-2 in Qingdao, the final result is the average of two  
241 accepted a-value solutions with six identified factors, including HOA, CCOA, COA, Aged-BBOA, LO-OOA and MO-OOA.  
242 Although the range of the O/C ratio of BBOA reported in Canagaratna et al. (2015) was from 0.25 to 0.55, fresh BBOA was  
243 found to be rapidly converted to OOA in less than 1 day (Bougiatioti et al., 2014), and the O/C ratio of aged BBOA could be  
244 up to 0.85 (Zheng et al., 2017). BBOA in Dongguan was apparently not fresh considering it is an urban site and Dongguan has  
245 a warmer winter (17 °C in Dongguan vs. 9 °C in Qingdao). The BBOA factor identified in Dongguan, with a strong contribution  
246 of m/z 60, had a higher O/C, indicating it was an oxygenated BBOA, therefore we name it Aged-BBOA in this study. All of  
247 the information regarding the final source results is shown in Figure 3b. Good correlations between each OA factor and their  
248 tracers indicate that the resolved ME-2 results are reasonable. A few sharp drops (which always occurred at approximately  
249 20:00) were observed in the MO-OOA time series ranging from December 29 to January 5, which coincides with extreme  
250 organic aerosol pollution (Figure S5). The inherent mechanisms for these drops remain unexplained, although we have tried a

251 number of reasonable approaches (e.g., splitting the period into sub-periods to identify the sources, constraining more factors  
252 before running ME-2, and examining more factors) to address this issue. A similar problem in the MO-OOA time series was  
253 also found in a recent ME-2 application (Qin et al., 2017). In our case, we presume this might be the result of relatively worse  
254 meteorological conditions at night during the sampling period, thereby increasing the contribution of late supper emissions  
255 and leading to the overestimation of COAs offset by drops in the MO-OOA concentration. Also note that the O/C ratios of the  
256 POAs in Dongguan were higher than those in Qingdao, suggesting that POA emissions in Dongguan underwent faster chemical  
257 processing. In addition, the relatively smaller contributions of POAs further support this inference. Freshly emitted POAs may  
258 get mixed with aged OAs more easily, while ME-2 may still consider them unmixed. MO-OOAs accounted for an average of  
259 42.8% of the total OA mass (which is much greater than the contribution of LO-OOAs), which is probably because some POA  
260 species could have been rapidly converted to very aged OOs (Bougiatioti et al., 2014; Xu et al., 2015). As mentioned above,  
261 the characteristics of the diurnal trends of the POA factors in Dongguan were similar to those in Qingdao, and thus, we focused  
262 on the OOA factors. MO-OOAs still showed higher concentrations during the daytime but, unlike LO-OOAs in Qingdao, the  
263 diurnal patterns of LO-OOAs in Dongguan were flat, implying that secondary OA formation in the LO-OOAs basically offset  
264 the influences of PBL variations.

265 Meteorological conditions (especially wind) play a crucial role in the dilution and transport of air pollution. We used the  
266 relationships between the component concentrations and wind to profoundly understand the origins of the OA factors and their  
267 nature. The distributions of the OA factor concentrations versus the wind direction and speed are plotted in Figure S7. For  
268 both of the urban sites, higher mass concentrations of the POA factors were mostly accompanied by low wind speeds, denoting  
269 their local emission characteristics. Additionally, for the OOA factors, a large proportion of their higher concentrations were  
270 maintained at higher wind speeds, indicating that the OOs were formed by transport processes. However, the small fraction  
271 of high-level OOs that was concentrated within the low wind-speed region represents the fast formation of OOs from some  
272 local POA.



273  
 274 **Figure 3.** Mass spectra of the OA factors, average fractions of the OA factors, diurnal variations of the OA factors and time  
 275 series of the OA factors identified by the ME-2 method for (a)Qingdao and (b) Dongguan.

## 4.2 Regression analysis for POA tracers

BC and PAHs are mainly derived from incomplete combustion processes (Schmidt and Noack, 2000; White, 1985), and thus, they were used as tracers for the POAs. In this study, the BC was directly measured by the AE-31, and the PAHs were quantified using the method developed by Bruns et al. (2015) based on AMS data. Both the BC and PAHs showed pronounced diurnal cycles similar to those of the POAs (see Figure S8). In addition, POAs are properly split into different subtypes via the ME-2 method, thereby providing the possibility to better understand the contributions of different POAs to BC and PAHs and to verify the POA source identification. In this section, we use a multi-linear regression method to analyze the POA factors for BC and PAHs.

Figure 4 shows the average contributions of OA sources to BC and PAHs in Qingdao and Dongguan. At both sites, HOAs were the dominant attribute of BC (51% for Qingdao and 40% for Dongguan) and CCOAs contributed the most to the PAHs (59% for Qingdao and 43% for Dongguan), indicating that BC mainly originates from traffic emissions and that PAHs in the Chinese urban polluted atmosphere are dominated by coal combustion during the wintertime. These findings are consistent with results reported in similar studies (Elser et al., 2016; Huang et al., 2015; Huang et al., 2010; Sun et al., 2016; Xu et al., 2014; Zhang et al., 2008). Moreover, the ratio of PAHs to OAs (1.8%) in Qingdao was similar to that in the northern Chinese urban site of Xi'an (1.9%) (Elser et al., 2016) but was higher than that in Dongguan (0.9%). This is likely because a larger fraction of coal combustion to the total OA concentration would enhance the ratio of PAHs to OAs (Elser et al., 2016). Biomass burning was the second-most important source for both BC and PAHs; it was responsible for 33% and 29% of the BC at Qingdao and Dongguan, respectively, and for 29% and 34% of the PAHs at Qingdao and Dongguan, respectively. Cooking emissions were a minor source of BC and PAHs, accounting for less than 10%. These results are also consistent with the published findings. For example, biomass burning is an important source for BC (Kondo et al., 2011; Reddy et al., 2002) and, in some regions with fewer traffic emissions, BC has the best correlation with BBOAs (Schwarz et al., 2008). In addition, in Beijing and California, PAHs are correlated well with BBOAs but are much more weakly correlated with COAs (Ge et al., 2012; Hu et al., 2016; Sun et al., 2016).

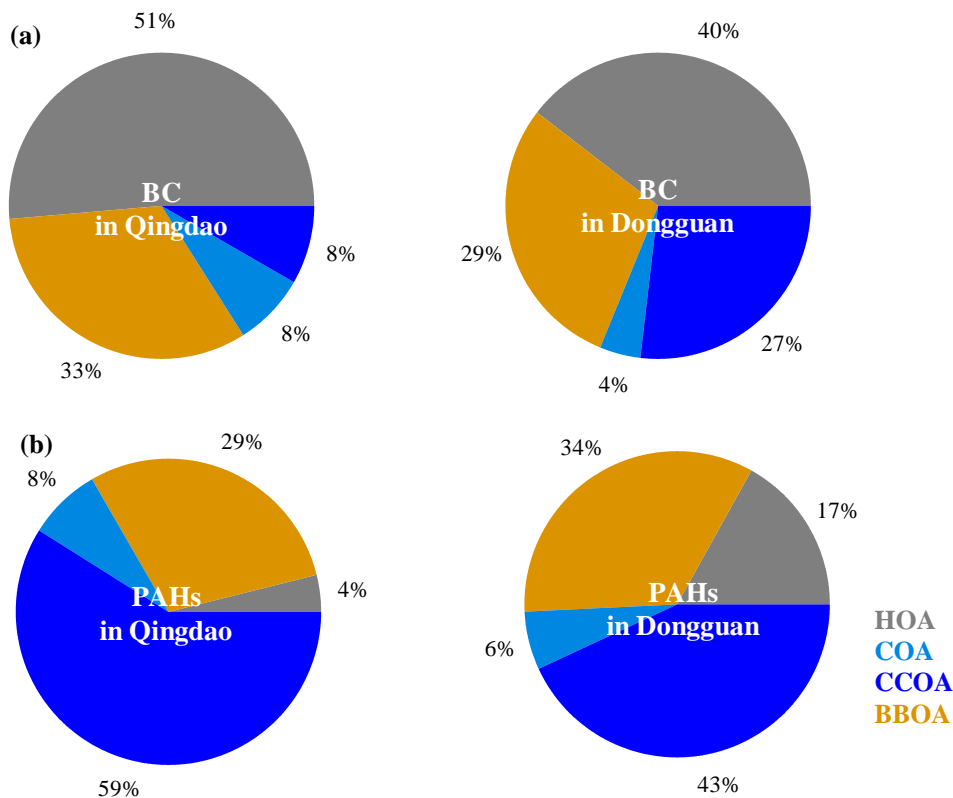


**Figure 4.** (a) Average contributions of POA factors to BC; (b) average contributions of POA factors to PAHs.

## 5 Conclusions

In this study, we used PMF to interpret the organic aerosol sources at two Chinese urban sites in winter, and found that PMF did not work properly (i.e., it did not allow for the separation of several primary sources of OAs). Therefore, we adopted the ME-2 approach, which yields more reliable solutions. Technically, there are three important steps when using the ME-2 method to interpret the sources of OAs. The first step is to investigate the mixed and unidentified factors that are constrained according to issues in the unconstrained PMF results. Generally, we constrained one or more POA factors (i.e., HOA, COA, BBOA and CCOA) for the polluted urban sites. The second step is to search for a reasonable anchor profile for each constrained factor. Two approaches were used: searching for anchor profiles via an increase in the number of unconstrained PMF factors from the same data set and using mass profiles derived from other similar studies. The third step is to choose the criteria for obtaining the optimal results. The choice of a reasonable range of O/C ratios may represent a good criterion for HR-OA apportionment since the O/C ratio is a significant and distinctive characteristic for different OA factors. In addition, correlations between the resolved OA factors and their tracers were also suggested.

314 **Acknowledgments**

315 This work was supported by the National Natural Science Foundation of China (91744202, U1301234), the Ministry of  
316 Science and Technology of China (2017YFC0210004), and the Science and Technology Plan of Shenzhen Municipality  
317 (JCYJ20170412150626172).

318 **References**

- 319 Aiken, A. C., D. Salcedo, M. J. Cubison, J. A. Huffman, P. F. DeCarlo, I. M. Ulbrich, K. S. Docherty, D. Sueper, J. R.  
320 Kimmel, D. R. Worsnop, A. Trimborn, M. Northway, E. A. Stone, J. J. Schauer, R. M. Volkamer, E. Fortner, B. de Foy,  
321 J. Wang, A. Laskin, V. Shutthanandan, J. Zheng, R. Zhang, J. Gaffney, N. A. Marley, G. Paredes-Miranda, W. P. Arnott,  
322 L. T. Molina, G. Sosa, and J. L. Jimenez : Mexico City aerosol analysis during MILAGRO using high resolution aerosol  
323 mass spectrometry at the urban supersite (T0) – Part 1: Fine particle composition and organic source apportionment,  
324 *Atmos. Chem. Phys.*, 9(17), 6633-6653, doi: 10.5194/acp-9-6633-2009,2009.
- 325 Alfarra, M. R., A. S. H. Prevot, S. Szidat, J. Sandradewi, S. Weimer, V. A. Lanz, D. Schreiber, M. Mohr, and U.  
326 Baltensperger : Identification of the Mass Spectral Signature of Organic Aerosols from Wood Burning Emissions,  
327 *Environ Sci. Technol.*, 41(16), 5770-5777, doi: 10.1021/es062289b,2007.
- 328 Allan, J. D., A. E. Delia, H. Coe, K. N. Bower, M. R. Alfarra, J. L. Jimenez, A. M. Middlebrook, F. Drewnick, T. B. Onasch,  
329 M. R. Canagaratna, J. T. Jayne, and D. R. Worsnop: A generalised method for the extraction of chemically resolved mass  
330 spectra from Aerodyne aerosol mass spectrometer data, *J. Aerosol Sci.*, 35(7), 909-922, doi:  
331 <https://doi.org/10.1016/j.jaerosci.2004.02.007>,2004.
- 332 Bougiatioti, A., I. Stavroulas, E. Kostenidou, P. Zarnmpas, C. Theodosi, G. Kouvarakis, F. Canonaco, A. S. H. Prévôt, A.  
333 Nenes, S. N. Pandis, and N. Mihalopoulos : Processing of biomass-burning aerosol in the eastern Mediterranean during  
334 summertime, *Atmos. Chem. Phys.*, 14(9), 4793-4807, doi: 10.5194/acp-14-4793-2014,2014.
- 335 Bruns, E. A., M. Krapf, J. Orasche, Y. Huang, R. Zimmermann, L. Drinovec, G. Močnik, I. El-Haddad, J. G. Slowik, J.  
336 Dommen, U. Baltensperger, and A. S. H. Prévôt : Characterization of primary and secondary wood combustion products  
337 generated under different burner loads, *Atmos. Chem. Phys.*, 15(5), 2825-2841, doi: 10.5194/acp-15-2825-2015,2015.
- 338 Canagaratna, M. R., J. L. Jimenez, J. H. Kroll, Q. Chen, S. H. Kessler, P. Massoli, L. Hildebrandt Ruiz, E. Fortner, L. R.  
339 Williams, K. R. Wilson, J. D. Surratt, N. M. Donahue, J. T. Jayne, and D. R. Worsnop : Elemental ratio measurements of  
340 organic compounds using aerosol mass spectrometry: characterization, improved calibration, and implications, *Atmos.*  
341 *Chem. Phys.*, 15(1), 253-272, doi: 10.5194/acp-15-253-2015,2015.
- 342 Canagaratna, M. R., J. T. Jayne, J. L. Jimenez, J. D. Allan, M. R. Alfarra, Q. Zhang, T. B. Onasch, F. Drewnick, H. Coe, A.  
343 Middlebrook, A. Delia, L. R. Williams, A. M. Trimborn, M. J. Northway, P. F. DeCarlo, C. E. Kolb, P. Davidovits, and

344 D. R. Worsnop : Chemical and microphysical characterization of ambient aerosols with the aerodyne aerosol mass  
345 spectrometer, *Mass Spectrom. Rev.*, 26(2), 185-222, doi: 10.1002/mas.20115,2007.

346 Canonaco, F., M. Crippa, J. G. Slowik, U. Baltensperger, and A. S. H. Prévôt : SoFi, an IGOR-based interface for the  
347 efficient use of the generalized multilinear engine (ME-2) for the source apportionment: ME-2 application to aerosol  
348 mass spectrometer data, *Atmos. Meas. Tech.*, 6(12), 3649-3661, doi: 10.5194/amt-6-3649-2013,2013.

349 Crippa, M., DeCarlo, P. F., Slowik, J. G., Mohr, C., Heringa, M.F., Chirico, R., Poulain, L., Freutel, F., Sciare, J., Cozic, J.,  
350 DiMarco, C. F., Elsasser, M., José, N., Marchand, N., Abidi, E., Wiedensohler, A., Drewnick, F., Schneider, J.,  
351 Borrmann, S., Nemitz, E., Zimmermann, R., Jaffrezo, J.-L., Prévôt, A. S. H., and Baltensperger, U.: Wintertime aerosol  
352 chemical composition and source apportionment of the organic fraction in the metropolitan area of Paris, *Atmos. Chem.  
353 Phys.*, 13, 961–981, doi:10.5194/acp-13-961-2013, 2013.

354 Crippa, M., F. Canonaco, V. a. Lanz, M. Äijälä, J. D. Allan, S. Carbone, G. Capes, D. Ceburnis, M. Dall'Osto, D. A. Day, P.  
355 F. DeCarlo, M. Ehn, a. Eriksson, E. Freney, L. Hildebrandt Ruiz, R. Hillamo, J. L. Jimenez, H. Junninen, A. Kiendler-  
356 Scharr, A. M. Kortelainen, M. Kulmala, A. Laaksonen, A. A. Mensah, C. Mohr, E. Nemitz, C. O'Dowd, J. Ovadnevaite,  
357 S. N. Pandis, T. Petäjä, L. Poulain, S. Saarikoski, K. Sellegri, E. Swietlicki, P. Tiitta, D. R. Worsnop, U. Baltensperger,  
358 and A. S. H. Prévôt: Organic aerosol components derived from 25 AMS data sets across Europe using a consistent ME-2  
359 based source apportionment approach, *Atmos. Chem. Phys.*, 14(12), 6159-6176, doi: 10.5194/acp-14-6159-2014, 2014.

360 Docherty, K. S., E. A. Stone, I. M. Ulbrich, P. F. DeCarlo, D. C. Snyder, J. J. Schauer, R. E. Peltier, R. J. Weber, S. M.  
361 Murphy, J. H. Seinfeld, B. D. Grover, D. J. Eatough, and J. L. Jimenez : Apportionment of Primary and Secondary  
362 Organic Aerosols in Southern California during the 2005 Study of Organic Aerosols in Riverside (SOAR-1), *Environ  
363 Sci. Technol.*, 42(20), 7655-7662, doi: 10.1021/es8008166,2008.

364 Drewnick, F., S. S. Hings, P. DeCarlo, J. T. Jayne, M. Gonin, K. Fuhrer, S. Weimer, J. L. Jimenez, K. L. Demerjian, S.  
365 Borrmann, and D. R. Worsnop : A New Time-of-Flight Aerosol Mass Spectrometer (TOF-AMS)—Instrument  
366 Description and First Field Deployment, *Aerosol Sci. Tech.*, 39(7), 637-658, doi: 10.1080/02786820500182040,2005.

367 Elser, M., R. J. Huang, R. Wolf, J. G. Slowik, Q. Wang, F. Canonaco, G. Li, C. Bozzetti, K. R. Daellenbach, Y. Huang, R.  
368 Zhang, Z. Li, J. Cao, U. Baltensperger, I. El-Haddad, and A. S. H. Prévôt : New insights into PM<sub>2.5</sub> chemical  
369 composition and sources in two major cities in China during extreme haze events using aerosol mass spectrometry,  
370 *Atmos. Chem. Phys.*, 16(5), 3207-3225, doi: 10.5194/acp-16-3207-2016,2016.

371 Fröhlich, R., V. Crenn, A. Setyan, C. A. Belis, F. Canonaco, O. Favez, V. Riffault, J. G. Slowik, W. Aas, M. Aijälä, A.  
372 Alastuey, B. Artiñano, N. Bonnaire, C. Bozzetti, M. Bressi, C. Carbone, E. Coz, P. L. Croteau, M. J. Cubison, J. K.  
373 Esser-Gietl, D. C. Green, V. Gros, L. Heikkinen, H. Herrmann, J. T. Jayne, C. R. Lunder, M. C. Minguillón, G. Močnik,  
374 C. D. O'Dowd, J. Ovadnevaite, E. Petralia, L. Poulain, M. Priestman, A. Ripoll, R. Sarda-Estève, A. Wiedensohler, U.  
375 Baltensperger, J. Sciare, and A. S. H. Prévôt : ACTRIS ACSM intercomparison – Part 2: Intercomparison of ME-2  
376 organic source apportionment results from 15 individual, co-located aerosol mass spectrometers, *Atmos. Meas. Tech.*,  
377 8(6), 2555-2576, doi: 10.5194/amt-8-2555-2015,2015.

378 Ge, X., A. Setyan, Y. Sun, and Q. Zhang : Primary and secondary organic aerosols in Fresno, California during wintertime:  
379 Results from high resolution aerosol mass spectrometry, *J. Geophys. Res.-Atmos.*, 117(D19), 161-169, doi:  
380 10.1029/2012JD018026,2012.

381 Hallquist, M., J. C. Wenger, U. Baltensperger, Y. Rudich, D. Simpson, M. Claeys, J. Dommen, N. M. Donahue, C. George,  
382 A. H. Goldstein, J. F. Hamilton, H. Herrmann, T. Hoffmann, Y. Iinuma, M. Jang, M. E. Jenkin, J. L. Jimenez, A.  
383 Kiendler-Scharr, W. Maenhaut, G. McFiggans, T. F. Mentel, A. Monod, A. S. H. Prévôt, J. H. Seinfeld, J. D. Surratt, R.  
384 Szmigielski, and J. Wildt : The formation, properties and impact of secondary organic aerosol: current and emerging  
385 issues, *Atmos. Chem. Phys.*, 9(14), 5155-5236, doi: 10.5194/acp-9-5155-2009,2009.

386 He, L. Y., Y. Lin, X. F. Huang, S. Guo, L. Xue, Q. Su, M. Hu, S. J. Luan, and Y. H. Zhang : Characterization of high-  
387 resolution aerosol mass spectra of primary organic aerosol emissions from Chinese cooking and biomass burning,  
388 *Atmos. Chem. Phys.*, 10(23), 11535-11543, doi: 10.5194/acp-10-11535-2010,2010.

389 Hofzumahaus, A., F. Rohrer, K. Lu, B. Bohn, T. Brauers, C.-C. Chang, H. Fuchs, F. Holland, K. Kita, Y. Kondo, X. Li, S.  
390 Lou, M. Shao, L. Zeng, A. Wahner, and Y. Zhang : Amplified Trace Gas Removal in the Troposphere, *Science*,  
391 324(5935), 1702, doi: 10.1126/science.1164566,2009.

392 Hu, W., M. Hu, W. Hu, J. L. Jimenez, B. Yuan, W. Chen, M. Wang, Y. Wu, C. Chen, Z. Wang, J. Peng, L. Zeng, and M.  
393 Shao : Chemical composition, sources, and aging process of submicron aerosols in Beijing: Contrast between summer  
394 and winter, *J. Geophys. Res.-Atmos.*, 121(4), 1955-1977, doi: 10.1002/2015JD024020,2016.

395 Hu, W. W., M. Hu, B. Yuan, J. L. Jimenez, Q. Tang, J. F. Peng, W. Hu, M. Shao, M. Wang, L. M. Zeng, Y. S. Wu, Z. H.  
396 Gong, X. F. Huang, and L. Y. He: Insights on organic aerosol aging and the influence of coal combustion at a regional  
397 receptor site of central eastern China, *Atmos. Chem. Phys.*, 13(19), 10095-10112, doi: 10.5194/acp-13-10095-2013,2013.

398 Huang, R. J., Y. Zhang, C. Bozzetti, K. F. Ho, J. J. Cao, Y. Han, K. R. Daellenbach, J. G. Slowik, S. M. Platt, F. Canonaco,  
399 P. Zotter, R. Wolf, S. M. Pieber, E. A. Brun, M. Crippa, G. Ciarelli, A. Piazzalunga, M. Schwikowski, G. Abbaszade, J.  
400 Schnelle-Kreis, R. Zimmermann, Z. An, S. Szidat, U. Baltensperger, I. El Haddad, and A. S. H. Prévôt: High secondary  
401 aerosol contribution to particulate pollution during haze events in China, *Nature*, 514(7521), 218-222, doi:  
402 10.1038/nature13774,2015.

403 Huang, X. F., L. Y. He, L. Xue, T. L. Sun, L. W. Zeng, Z. H. Gong, M. Hu, and T. Zhu: Highly time-resolved chemical  
404 characterization of atmospheric fine particles during 2010 Shanghai World Expo, *Atmos. Chem. Phys.*, 12(11), 4897-  
405 4907, doi: 10.5194/acp-12-4897-2012,2012.

406 Huang, X. F., L. Y. He, M. Hu, M. R. Canagaratna, Y. Sun, Q. Zhang, T. Zhu, L. Xue, L. W. Zeng, X. G. Liu, Y. H. Zhang,  
407 J. T. Jayne, N. L. Ng, and D. R. Worsnop : Highly time-resolved chemical characterization of atmospheric submicron  
408 particles during 2008 Beijing Olympic Games using an Aerodyne High-Resolution Aerosol Mass Spectrometer, *Atmos.*  
409 *Chem. Phys.*, 10(18), 8933-8945, doi: 10.5194/acp-10-8933-2010,2010.



410 IPCC , Climate Change 2013: The Physical Science Basis. Contribution of Working Group I to the Fifth Assessment Report  
411 of the Intergovernmental Panel on Climate Change, 1535 pp., Cambridge University Press, Cambridge, United Kingdom  
412 and New York, NY, USA,2013.

413 Jayne, J. T., D. C. Leard, X. Zhang, P. Davidovits, K. A. Smith, C. E. Kolb, and D. R. Worsnop: Development of an Aerosol  
414 Mass Spectrometer for Size and Composition Analysis of Submicron Particles, *Aerosol Sci. Tech.*, 33(1-2), 49-70, doi:  
415 10.1080/027868200410840,2000.

416 Jimenez, J. L., M. R. Canagaratna, N. M. Donahue, A. S. H. Prevot, Q. Zhang, J. H. Kroll, P. F. DeCarlo, J. D. Allan, H.  
417 Coe, N. L. Ng, A. C. Aiken, K. S. Docherty, I. M. Ulbrich, A. P. Grieshop, A. L. Robinson, J. Duplissy, J. D. Smith, K.  
418 R. Wilson, V. A. Lanz, C. Hueglin, Y. L. Sun, J. Tian, A. Laaksonen, T. Raatikainen, J. Rautiainen, P. Vaattovaara, M.  
419 Ehn, M. Kulmala, J. M. Tomlinson, D. R. Collins, M. J. Cubison, J. Dunlea, J. A. Huffman, T. B. Onasch, M. R. Alfarra,  
420 P. I. Williams, K. Bower, Y. Kondo, J. Schneider, F. Drewnick, S. Borrmann, S. Weimer, K. Demerjian, D. Salcedo, L.  
421 Cottrell, R. Griffin, A. Takami, T. Miyoshi, S. Hatakeyama, A. Shimono, J. Y. Sun, Y. M. Zhang, K. Dzepina, J. R.  
422 Kimmel, D. Sueper, J. T. Jayne, S. C. Herndon, A. M. Trimborn, L. R. Williams, E. C. Wood, A. M. Middlebrook, C. E.  
423 Kolb, U. Baltensperger, and D. R. Worsnop : Evolution of Organic Aerosols in the Atmosphere, *Science*, 326(5959),  
424 1525-1529, doi: 10.1126/science.1180353,2009.

425 Kondo, Y., H. Matsui, N. Moteki, L. Sahu, N. Takegawa, M. Kajino, Y. Zhao, M. J. Cubison, J. L. Jimenez, S. Vay, G. S.  
426 Diskin, B. Anderson, A. Wisthaler, T. Mikoviny, H. E. Fuelberg, D. R. Blake, G. Huey, A. J. Weinheimer, D. J. Knapp,  
427 and W. H. Brune:Emissions of black carbon, organic, and inorganic aerosols from biomass burning in North America  
428 and Asia in 2008, *J. Geophys. Res.-Atmos.*, 116(D8), 353-366, doi: 10.1029/2010JD015152,2011.

429 Lanz, V. A., M. R. Alfarra, U. Baltensperger, B. Buchmann, C. Hueglin, and A. S. H. Prévôt : Source apportionment of  
430 submicron organic aerosols at an urban site by factor analytical modelling of aerosol mass spectra, *Atmos. Chem. Phys.*,  
431 7(6), 1503-1522, doi: 10.5194/acp-7-1503-2007,2007.

432 Lanz, V. A., A. S. H. Prévôt, M. R. Alfarra, S. Weimer, C. Mohr, P. F. DeCarlo, M. F. D. Gianini, C. Hueglin, J. Schneider,  
433 O. Favez, B. D'Anna, C. George, and U. Baltensperger: Characterization of aerosol chemical composition with aerosol  
434 mass spectrometry in Central Europe: an overview, *Atmos. Chem. Phys.*, 10(21), 10453-10471, doi: 10.5194/acp-10-  
435 10453-2010,2010.

436 Matthew, B. M., A. M. Middlebrook, and T. B. Onasch : Collection Efficiencies in an Aerodyne Aerosol Mass Spectrometer  
437 as a Function of Particle Phase for Laboratory Generated Aerosols, *Aerosol Sci. Tech.*, 42(11), 884-898, doi:  
438 10.1080/02786820802356797,2008.

439 Middlebrook, A. M., R. Bahreini, J. L. Jimenez, and M. R. Canagaratna : Evaluation of Composition-Dependent Collection  
440 Efficiencies for the Aerodyne Aerosol Mass Spectrometer using Field Data, *Aerosol Sci. Tech.*, 46(3), 258-271, doi:  
441 10.1080/02786826.2011.620041,2012.

442 Mohr, C., P. F. DeCarlo, M. F. Heringa, R. Chirico, J. G. Slowik, R. Richter, C. Reche, A. Alastuey, X. Querol, R. Seco, J.  
443 Peñuelas, J. L. Jiménez, M. Crippa, R. Zimmermann, U. Baltensperger, and A. S. H. Prévôt : Identification and

444 quantification of organic aerosol from cooking and other sources in Barcelona using aerosol mass spectrometer data,  
445 *Atmos. Chem. Phys.*, 12(4), 1649-1665, doi: 10.5194/acp-12-1649-2012,2012.

446 Ng, N. L., M. R. Canagaratna, J. L. Jimenez, Q. Zhang, I. M. Ulbrich, and D. R. Worsnop : Real-Time Methods for  
447 Estimating Organic Component Mass Concentrations from Aerosol Mass Spectrometer Data, *Environ Sci. Technol.*,  
448 45(3), 910-916, doi: 10.1021/es102951k,2011.

449 Paatero, P. :The Multilinear Engine: A Table-Driven, Least Squares Program for Solving Multilinear Problems, including  
450 the n-Way Parallel Factor Analysis Model, *J. Comput. Graph. Stat.*, 8(4), 854-888, doi: 10.2307/1390831,1999.

451 Paatero, P., and U. Tapper : Positive matrix factorization: A non-negative factor model with optimal utilization of error  
452 estimates of data values, *Environmetrics*, 5(2), 111-126, doi: 10.1002/env.3170050203,1994.

453 Pope, C. A., and D. W. Dockery : Health Effects of Fine Particulate Air Pollution: Lines that Connect, *J. Air Waste*  
454 *Manage.*,56(6), 709-742, doi: 10.1080/10473289.2006.10464485,2006.

455 Pratt, K. A., and K. A. Prather : Mass spectrometry of atmospheric aerosols—Recent developments and applications. Part II:  
456 On-line mass spectrometry techniques, *Mass Spectrom. Rev.*, 31(1), 17-48, doi: 10.1002/mas.20330,2012.

457 Qin, Y. M., H. B. Tan, Y. J. Li, M. I. Schurman, F. Li, F. Canonaco, A. S. H. Prévôt, and C. K. Chan : Impacts of traffic  
458 emissions on atmospheric particulate nitrate and organics at a downwind site on the periphery of Guangzhou, China,  
459 *Atmos. Chem. Phys.*, 17(17), 10245-10258, doi: 10.5194/acp-17-10245-2017,2017.

460 Reddy, C. M., A. Pearson, L. Xu, A. P. McNichol, B. A. Benner, S. A. Wise, G. A. Klouda, L. A. Currie, and T. I.  
461 Eglinton :Radiocarbon as a Tool To Apportion the Sources of Polycyclic Aromatic Hydrocarbons and Black Carbon in  
462 Environmental Samples, *Environ Sci. Technol.*, 36(8), 1774-1782, doi: 10.1021/es011343f,2002.

463 Reyes-Villegas, E., D. C. Green, M. Priestman, F. Canonaco, H. Coe, A. S. H. Prévôt, and J. D. Allan: Organic aerosol  
464 source apportionment in London 2013 with ME-2: exploring the solution space with annual and seasonal analysis,  
465 *Atmos. Chem. Phys.*, 16(24), 15545-15559, doi: 10.5194/acp-16-15545-2016,2016.

466 Schmidt, M. W. I., and A. G. Noack : Black carbon in soils and sediments: Analysis, distribution, implications, and current  
467 challenges, *Global Biogeochem. Cy.*, 14(3), 777-793, doi: 10.1029/1999GB001208,2000.

468 Schwarz, J. P., R. S. Gao, J. R. Spackman, L. A. Watts, D. S. Thomson, D. W. Fahey, T. B. Ryerson, J. Peischl, J. S.  
469 Holloway, M. Trainer, G. J. Frost, T. Baynard, D. A. Lack, J. A. de Gouw, C. Warneke, and L. A. Del  
470 Negro :Measurement of the mixing state, mass, and optical size of individual black carbon particles in urban and biomass  
471 burning emissions, *Geophys Res. Lett.*, 35(13), L13810, doi: 10.1029/2008GL033968,2008.

472 Sun, Y., W. Du, P. Fu, Q. Wang, J. Li, X. Ge, Q. Zhang, C. Zhu, L. Ren, W. Xu, J. Zhao, T. Han, D. R. Worsnop, and Z.  
473 Wang : Primary and secondary aerosols in Beijing in winter: sources, variations and processes, *Atmos. Chem. Phys.*,  
474 16(13), 8309-8329, doi: 10.5194/acp-16-8309-2016,2016.

475 Tian, H., Cheng, K., Wang, Y., Zhao, D., Lu, L., Jia, W. and Hao, J.: Temporal and spatial variation characteristics of  
476 atmospheric emissions of Cd, Cr, and Pb from coal in China. *Atmospheric Environment*, 50: 157-163,doi:  
477 10.1016/j.atmosenv.2011.12.045,2012.

478 Ulbrich, I. M., M. R. Canagaratna, Q. Zhang, D. R. Worsnop, and J. L. Jimenez : Interpretation of organic components from  
479 Positive Matrix Factorization of aerosol mass spectrometric data, *Atmos. Chem. Phys.*, 9(9), 2891-2918, doi:  
480 10.5194/acp-9-2891-2009,2009.

481 Wang, X., B. J. Williams, X. Wang, Y. Tang, Y. Huang, L. Kong, X. Yang, and P. Biswas: Characterization of organic  
482 aerosol produced during pulverized coal combustion in a drop tube furnace, *Atmos. Chem. Phys.*, 13(21), 10919-10932,  
483 doi: 10.5194/acp-13-10919-2013,2013.

484 White, H. :Black carbon in the environment, J. Wiley,1985.

485 Xu, J., Q. Zhang, M. Chen, X. Ge, J. Ren, and D. Qin: Chemical composition, sources, and processes of urban aerosols  
486 during summertime in northwest China: insights from high-resolution aerosol mass spectrometry, *Atmos. Chem. Phys.*,  
487 14(23), 12593-12611, doi: 10.5194/acp-14-12593-2014,2014.

488 Xu, L., S. Suresh, H. Guo, R. J. Weber, and N. L. Ng : Aerosol characterization over the southeastern United States using  
489 high-resolution aerosol mass spectrometry: spatial and seasonal variation of aerosol composition and sources with a  
490 focus on organic nitrates, *Atmos. Chem. Phys.*, 15(13), 7307-7336, doi: 10.5194/acp-15-7307-2015,2015.

491 Zhang, Q., J. L. Jimenez, M. R. Canagaratna, I. M. Ulbrich, N. L. Ng, D. R. Worsnop, and Y. Sun : Understanding  
492 atmospheric organic aerosols via factor analysis of aerosol mass spectrometry: a review, *Anal. Bioanal. Chem.*, 401(10),  
493 3045-3067, doi: 10.1007/s00216-011-5355-y,2011.

494 Zhang, Q., J. L. Jimenez, M. R. Canagaratna, J. D. Allan, H. Coe, I. Ulbrich, M. R. Alfarra, A. Takami, A. M. Middlebrook,  
495 Y. L. Sun, K. Dzepina, E. Dunlea, K. Docherty, P. F. DeCarlo, D. Salcedo, T. Onasch, J. T. Jayne, T. Miyoshi, A.  
496 Shimono, S. Hatakeyama, N. Takegawa, Y. Kondo, J. Schneider, F. Drewnick, S. Borrmann, S. Weimer, K. Demerjian,  
497 P. Williams, K. Bower, R. Bahreini, L. Cottrell, R. J. Griffin, J. Rautiainen, J. Y. Sun, Y. M. Zhang, and D. R.  
498 Worsnop :Ubiquity and dominance of oxygenated species in organic aerosols in anthropogenically-influenced Northern  
499 Hemisphere midlatitudes, *Geophys. Res. Lett.*, 34(13), L13801, doi: 10.1029/2007GL029979,2007.

500 Zhang, Y., J. J. Schauer, Y. Zhang, L. Zeng, Y. Wei, Y. Liu, and M. Shao : Characteristics of Particulate Carbon Emissions  
501 from Real-World Chinese Coal Combustion, *Environ Sci. Technol.*, 42(14), 5068-5073, doi: 10.1021/es7022576,2008.

502 Zhou, S., S. Collier, D. A. Jaffe, N. L. Briggs, J. Hee, A. J. Sedlacek Iii, L. Kleinman, T. B. Onasch, and Q. Zhang :  
503 Regional influence of wildfires on aerosol chemistry in the western US and insights into atmospheric aging of biomass  
504 burning organic aerosol, *Atmos. Chem. Phys.*, 17(3), 2477-2493, doi: 10.5194/acp-17-2477-2017,2017.

505

# Improved source apportionment of organic aerosols in complex urban air pollution using the multilinear engine (ME-2)

Qiao Zhu<sup>1</sup>, Xiao-Feng Huang<sup>1,\*</sup>, Li-Ming Cao<sup>1</sup>, Lin-Tong Wei<sup>1</sup>, Bin Zhang<sup>1</sup>, Ling-Yan He<sup>1</sup>, Miriam Elser<sup>2</sup>, Francesco Canonaco<sup>2</sup>, Jay G. Slowik<sup>2</sup>, Carlo Bozzetti<sup>2</sup>, Imad El-Haddad<sup>2</sup>, and André S.H. Prévôt<sup>2</sup>

<sup>1</sup>Key Laboratory for Urban Habitat Environmental Science and Technology, School of Environment and Energy, Peking University Shenzhen Graduate School, Shenzhen, 518055, China.

<sup>2</sup>Paul Scherrer Institute (PSI), 5232 Villigen-PSI, Switzerland

**Abstract** Organic aerosols (OAs), which consist of thousands of complex compounds emitted from various sources, constitute one of the major components of fine particulate matter. The traditional positive matrix factorization (PMF) method often apportions aerosol mass spectrometer (AMS) organic datasets into less meaningful or mixed factors, especially in complex urban cases. In this study, an improved source apportionment method using a bilinear model of the multilinear engine (ME-2) was applied to OAs collected during the heavily polluted season from two Chinese megacities located in the north and south with an Aerodyne high-resolution aerosol mass spectrometer (HR-ToF-AMS). We applied a rather novel procedure for utilization of prior information and selecting optimal solutions, which does not necessarily depend on other studies. Ultimately, six reasonable factors were clearly resolved and quantified for both sites by constraining one or more factors: hydrocarbon-like OA (HOA), cooking-related OA (COA), biomass burning OA (BBOA), coal combustion (CCOA), less-oxidized oxygenated OA (LO-OOA) and more-oxidized oxygenated OA (MO-OOA). In comparison, the traditional PMF method could not effectively resolve the appropriate factors, e.g., BBOA and CCOA, in the solutions. Moreover, coal combustion and traffic emissions were determined to be primarily responsible for the concentrations of PAHs and BC, respectively, through the regression analyses of the ME-2 results.

## 1 Introduction

Atmospheric aerosols are generating increasing interest due to their adverse effects on human health, visibility and the climate (IPCC, 2013; Pope and Dockery, 2006). Among different particulate compositions, many studies focus on organic aerosols (OAs) because they contribute 20-90% to the total submicron mass (Jimenez et al., 2009; Zhang et al., 2007). OAs can be either directly emitted by various sources, including anthropogenic (i.e., traffic and combustion activities) and biogenic sources, or produced via secondary formation after the oxidation of volatile organic compounds (VOCs) (Hallquist et al., 2009).

---

<sup>1</sup> Correspondence to: X.-F. Huang (huangxf@pku.edu.cn)

27 Therefore, the reliable source identification and quantification of OAs are essential before developing effective political  
28 abatement strategies.

29 Aerodyne aerosol mass spectrometer (AMS) systems are the most widely adopted on-line aerosol measurement systems  
30 for acquiring aerosol chemical compositions (Canagaratna et al., 2007; Pratt and Prather, 2012). An AMS provides on-line  
31 quantitative mass spectra of non-refractory components from the submicron aerosol fraction with a high temporal resolution  
32 (i.e., seconds to minutes) (Canagaratna et al., 2007). The total mass spectra can be assigned to both several inorganic  
33 compounds and the organic fraction through mass spectral fragmentation tables (Allan et al., 2004). To further investigate the  
34 different types of organic fractions, numerous studies have exploited the positive matrix factorization (PMF) algorithm and  
35 apportioned the AMS organic mass spectra in terms of their source emissions or formation processes (Zhang et al., 2011).  
36 PMF is a standard multivariate factor analysis tool (Paatero, 1999; Paatero and Tapper, 1994) that models the time series of  
37 measured organic mass spectra as a linear combination of positive factor profiles and their respective time series. Most of the  
38 earlier PMF studies were conducted on unit-mass resolution (UMR) mass spectrometers (Lanz et al., 2007; Lanz et al., 2010;  
39 Ulbrich et al., 2009), although more have recently focused on high-resolution (HR) mass spectra PMF (Aiken et al., 2009;  
40 Docherty et al., 2008; Huang et al., 2010). The use of HR mass spectra data to constrain PMF solutions can reduce their  
41 rotational ambiguity and result in more interpretable OA factors. For example, Aiken et al. (2009) found that hydrocarbon-like  
42 OA (HOA) and biomass burning OA (BBOA) were better separated using HR-AMS data than with UMR data. However, even  
43 HR-AMS-PMF can also yield mixed factors (especially in heavily polluted areas) due to their complex emission patterns.

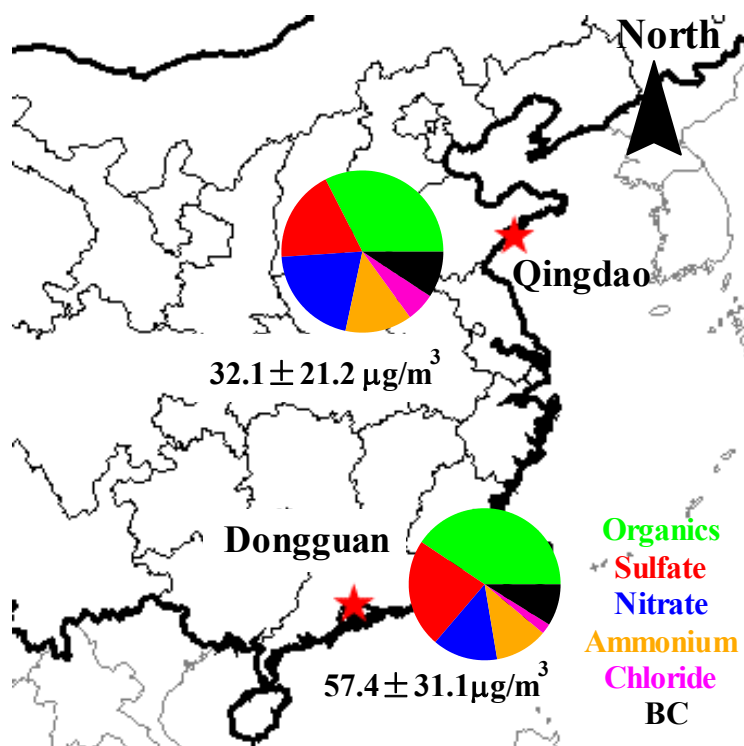
44 The abundant characteristic fragments for cooking-related OA (COA) (e.g.,  $m/z$  55 and 57) and coal combustion OA  
45 (CCOA) (e.g.,  $m/z$  51, 53, and 65) can be observed in the mass spectrum of the HOA factor (He et al., 2010; Hu et al., 2013).  
46 Elser et al., 2016) analyzed two urban HR-AMS datasets in China, and their PMF results showed an HOA profile that  
47 contained a high concentration of  $C_2H_4O_2^+$  ( $m/z$  60), which is a BBOA tracer ion. In addition,  $CO_2^+$  ( $m/z$  44) contributed more  
48 to COA compared to oxygenated OA (OOA). To solve this “mixed factor” problem in PMF analysis, some researchers  
49 attempted to use the multilinear engine algorithm (ME-2) with user-provided constraints (Canonaco et al., 2013; Crippa et al.,  
50 2014; Elser et al., 2016; Reyes-Villegas et al., 2016). However, several key issues with the ME-2 in these studies, such as  
51 reliability of the user-input constraints and the criteria used to determine an optimal result, still require further investigation.  
52 Most ME-2 studies (Crippa et al., 2014; Elser et al., 2016; Reyes-Villegas et al., 2016) were based on HR-AMS datasets and  
53 utilized mass profiles of PMF results from Paris (Crippa et al., 2013; mostly due to the lack of other reliable source profiles)  
54 and did not consider the specific sampling sites, which could result in uncertainties.

55 In this study, a novel source apportionment technique using the multi-linear engine tool (ME-2) was successfully applied  
56 to organic mass spectra obtained with an HR-ToF-AMS at two urban sites during pollution-heavy periods during the same  
57 year. The improved OA source apportionment results are discussed and compared with an unconstrained PMF analysis.

59 **2.1 Sampling sites and period**

60 Measurements at Qingdao (36.10°N, 120.47°E, 10 m above ground level, a.g.l.) were performed from 1 to 31 November  
61 2013, while those in Dongguan were conducted from 12 December 2013 to 1 January 2014 (33.03°N, 113.75°E, 100 m a.g.l.).  
62 Qingdao is a coastal city with over 9 million inhabitants in northern China, while Dongguan has over 8 million inhabitants and  
63 is located in southern China (shown in Figure 1). Both of the sampling sites are on the tops of buildings in urban central areas,  
64 and there is no industrial emission nearby.

65



66

67 **Figure 1.** The locations and the average PM<sub>1</sub> chemical compositions of the Qingdao and Dongguan sampling sites.

68 **2.2 Instrumentation**

69 An HR-ToF-AMS was deployed for the on-line measurement of non-refractory PM<sub>1</sub> (Canagaratna et al., 2007). The setup  
70 and operation of the HR-ToF-AMS was similar to that in our previous studies (Huang et al., 2015; Huang et al., 2010). A PM<sub>2.5</sub>  
71 cyclone inlet was briefly placed on the roof of a building to remove coarse particles and to introduce an air stream containing  
72 the remaining particles into a room through a copper tube with a flow rate of  $10 \text{ l min}^{-1}$ . A nafion dryer (MD-070-12S-4, Perma  
73 Pure Inc.) was positioned upstream of the HR-ToF-AMS to eliminate the potential influence of relative humidity on the

74 particle collection (Matthew et al., 2008), after which the HR–ToF–AMS isokinetically sampled from the center of the copper  
75 tube at a flow rate of 80 ml min<sup>-1</sup>. The instrument was operated at two ion optical modes with a cycle of 4 min, including 2  
76 min for the mass-sensitive V-mode and 2 min for the high mass resolution W-mode. An aethalometer (AE-31, Magee), which  
77 also has a PM<sub>2.5</sub> inlet, was simultaneously used for measurements of refractory black carbon (BC) with a temporal resolution  
78 of 5 min.

79 A routine analysis of the HR–ToF–AMS data was performed using the software SQUIRREL (version 1.57) and PIKA  
80 (version 1.16) written in Igor Pro 6.37 (Wave Metrics  
81 Inc.)(<http://cires1.colorado.edu/jimenezgroup/ToFAMSResources/ToFSoftware/index.html>). The ionization efficiency (IE)  
82 was calibrated using pure ammonium nitrate particles following standard protocols (Drewnick et al., 2005; Jayne et al.,  
83 2000). The relative IEs (RIEs) for organics, nitrate and chloride were assumed to be 1.4, 1.1 and 1.3, respectively. A  
84 composition-dependent collection efficiency (CE) was applied to the data based on the method of Middlebrook et al. (2012)  
85 and an organic elemental analysis was performed using the latest approach recommended by Canagaratna et al. (2015).

### 86 **2.3 PMF and ME-2 methods for OA source apportionment**

87 PMF is a mathematical technique used to solve bilinear unmixing problems (Paatero and Tapper, 1994) that enables a  
88 description of the variability of a multivariate database as the linear combination of static factor profiles and their  
89 corresponding time series. The bilinear factor analytic model in matrix notation is defined in Eq. (1), where the measured  
90 matrix X (consisting of i rows and j columns) is approximated by the product of G (containing the factor time series) and F  
91 (the factor profiles). E denotes the model residuals. The entries in G and F are fitted using a least-squares algorithm that  
92 iteratively minimizes the quantity Q (Eq. 2), which is defined as the sum of the squared residuals (e<sub>ij</sub>) weighted by their  
93 respective uncertainties (σ<sub>ij</sub>).

$$94 \quad X = G \times F + E \quad (1)$$

$$95 \quad Q = \sum_{i=1}^m \sum_{j=1}^n \left( \frac{e_{ij}}{\sigma_{ij}} \right)^2 \quad (2)$$

96 In this study, we adopted SoFi (Canonaco et al., 2013), which is an implementation of the multilinear engine (ME-2)  
97 (Paatero, 1999), to perform the organic HR-AMS data analysis. In contrast to an unconstrained PMF analysis, ME-2 enables  
98 a more complete exploration of the rotational ambiguity of the solution space. In our case, this is achieved by directing the  
99 solution towards environmentally meaningful rotations using the *a* value approach. This method uses prior input profiles and  
100 the scalar *a* to constrain one or more output factor profiles such that they fall within a predetermined range. The *a* value  
101 determines the extent to which the output profiles are allowed to vary from the input profiles according to Eq. (3), where *f*  
102 represents the factor profile and *j* indicates the *m/z* of the ions.

$$103 \quad f_{j,\text{solution}} = f_j \pm a \times f_j \quad (3)$$

104 The number of output factors, which is selected by the user, is a key consideration for PMF analysis. Most unconstrained PMF  
105 results were chosen following the procedures detailed in Zhang et al. (2007). However, additional outputs in ME-2 can be

106 generated to explore more of the solution space, and more criteria should be developed to support the factor identification,  
107 which will be discussed in section 3.

## 108 **2.4 Polycyclic aromatic hydrocarbons (PAHs) quantification**

109 In this study, PAHs mass concentrations were quantitatively determined from the HR-AMS data. The steps outlined are  
110 as follows: first, the PAHs molecular ions  $[M]^+$ , including  $[C_{10}H_8]^+$ ,  $[C_{12}H_8]^+$ ,  $[C_{14}H_8]^+$ ,  $[C_{14}H_{10}]^+$ ,  $[C_{16}H_{10}]^+$ ,  $[C_{18}H_{10}]^+$ ,  
111  $[C_{18}H_{12}]^+$ ,  $[C_{20}H_{12}]^+$ ,  $[C_{22}H_{12}]^+$ ,  $[C_{22}H_{14}]^+$ ,  $[C_{24}H_{12}]^+$ ,  $[C_{24}H_{14}]^+$ , and other associated fragments, including  $[M-H]^+$ ,  $[M-2H]^+$ ,  
112  $[M]^{2+}$ , and  $[M-H]^{2+}$  were fitted in the HR spectra. Second, the fragments presented low correlation (i.e.,  $R^2$  below 0.6) with  
113 their corresponding molecular ions were not taken into account. Finally, the relative ionization efficiency (RIE) for PAHs was  
114 assumed to be 1.4 and the dependency of the collection efficiency ( $CE_b$ ) on the chemical composition of the aerosol was  
115 estimated using a composition-dependent collection efficiency (CDCE) algorithm (Middlebrook et al., 2012). More details  
116 about the method can be found in Bruns et al. (2015).

## 117 **3 Interpretation of OA source apportionment using ME-2**

118 In this section, a conventional PMF without any prior information is performed to analyze the OA source apportionment.  
119 Then, we use the ME-2 method to optimize the OA source apportionment based on the information obtained from the PMF  
120 method. The sequential steps are reported below:

### 121 1. Unconstrained PMF runs.

122 We performed unconstrained runs with a range from two to ten factors. Generally, PMF solutions with large numbers of  
123 factors are not considered due to possible mathematical splits of the factor profiles. However, some factors that have small  
124 contributions or that have similar mass profiles as other factors (but different time series) may only be found in solutions with  
125 large numbers of factors. We observe that most of the solutions provided via PMF include either multiply split factors or mixed  
126 factors that are not properly separated from one another. In other words, PMF does not produce an appropriate solution. The  
127 6-factor solutions for Qingdao and Dongguan are shown in Figure S1 and S2, and three types of primary OAs (POAs) were  
128 identified for each sampling site, including HOA), coal combustion OA (CCOA) and cooking OA (COA) for Qingdao and  
129 HOA, biomass burning OA (BBOA) and COA for Dongguan. Oxygenated OA (OOA) seems to be excessively split in the 6-  
130 factor solutions for both of the sites. HOA is distinguished by alkyl fragment signatures with prominent contributions of  $m/z$   
131 55 ( $C_4H_7^+$ ) and  $m/z$  57 ( $C_4H_9^+$ ) (Ng et al., 2011). The COA profile is similar to that of HOA but has a higher contribution from  
132 oxygenated ions at  $m/z$  55 ( $C_3H_3O^+$ ) and  $m/z$  57 ( $C_3H_5O^+$ ) (Mohr et al., 2012). BBOA is characterized by the presence of  
133 signals at  $m/z$  60 ( $C_2H_4O_2^+$ ) and  $m/z$  73 ( $C_3H_5O_2^+$ ), which are identified as fragments from anhydrous sugars present in biomass  
134 smoke (Alfarra et al., 2007). The OOA profile is characterized by a high signal at  $m/z$  44 ( $CO_2^+$ ). Note that some POA profiles  
135 in this solution indicate mixing; for example, CCOAs in Qingdao contain a high concentration of the biomass burning tracer  
136 ion ( $m/z$  60,  $C_2H_4O_2^+$ ), and HOAs in Dongguan have a higher-than-expected contribution of  $m/z$  44 ( $CO_2^+$ ) with a high O/C



137 ratio (0.26). In addition, CCOA seems to be mixed with BBOA. We then further verified the solutions with additional factors.  
138 The results show that BBOA and CCOA are separated from each other in the 7- and 8-factor solutions for Qingdao (see Figure  
139 S1) and that better signals for unmixed and stable HOA with low O/C ratios of 0.17 or 0.18 emerged in the 7- to 10-factor  
140 solutions for Dongguan (see Figure S2).

## 141 2. Investigate anchor profiles for ME-2.

142 Before operating ME-2, feasible and reasonable prior input profiles must be determined. To the best of our knowledge,  
143 this is the first HR-OA data set that employs anchor profiles extracted from an unconstrained PMF solution with a higher  
144 number of factors, and the same approach has been successfully applied to source apportionment efforts using UMR ME-2  
145 (Fröhlich et al., 2015). In our case for Qingdao, the BBOA anchor profile should be investigated, and we attempted to look for  
146 it from the unconstrained PMF results based on the same dataset, and found that the BBOA factors in the 7- and 8-factor  
147 solutions might be used as the anchor profiles. They both had good correlation with the BBOA MS in Chinese biomass burning  
148 emission simulation (He et al., 2010), confirming their basic BBOA characteristics. Although these two BBOA factors are  
149 quite similar, the BBOA from the 8-factor solution is better suited to be a constraining profile due to its smaller  $m/z$  44 ( $\text{CO}_2^+$ )  
150 signal and higher  $m/z$  60 ( $\text{C}_2\text{H}_4\text{O}_2^+$ ) signal (see Figure S3). In addition, the BBOA from the 8-factor solution also correlates  
151 better with the BBOA from a Chinese biomass burning simulation ( $R^2=0.81$ ) than the 7-factor solution ( $R^2=0.79$ ). For  
152 Dongguan, the anchor profile for HOA can be obtained from unconstrained PMF solutions. The averaged HOA profile from  
153 the 7- to 10-factor solutions was used as the anchor profile for ME-2 due to the small differences among the different solutions.  
154 Additionally, the constraining CCOA profile for Dongguan is still under consideration because the mass spectrum of BBOA  
155 was found to be very similar to that of CCOA, raising the concern that coal combustion particles might have been incorrectly  
156 apportioned to biomass burning sources (Wang et al., 2013). An appropriate CCOA anchor profile could not be obtained due  
157 to an increase in the unconstrained PMF factor number (see Figure S2). The best approach is to employ the CCOA profile  
158 from Qingdao as the constraining profile for Dongguan in ME-2, as these two campaigns were conducted using the same HR-  
159 ToF-AMS in the same year. In addition, the CCOA from Qingdao has a very good correlation ( $R^2=0.97$ ) with CCOA profiles  
160 reported at other Chinese urban sites (Elser et al., 2016) (see Figure S4). Tian et al. (2012) also found that the emission  
161 compositions of coal combustion in different regions in China are quite similar. The input profiles for BBOA, HOA and CCOA  
162 prior to operating ME-2 are shown in Figure 2.

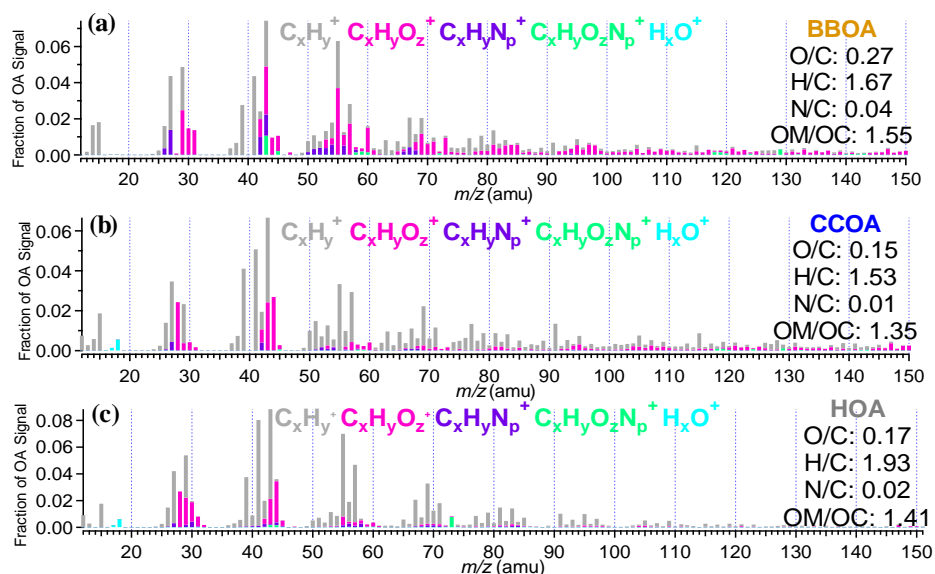


**Figure 2.** The anchor mass spectra for (a) BBOA, (b) CCOA and (c) HOA in the ME-2 analysis.

3. Constrain the mass spectrums of the mixed factors with different  $a$  values.

According to the unconstrained PMF results, the best interpretable results for both two sites are the 6-factor solutions with factors that include HOA, COA, BBOA, CCOA, less-oxidized oxygenated OA (LO-OOA) and more-oxidized oxygenated OA (MO-OOA) (Figure 3a and 3b). The  $a$  values set from 0 to 1 with an increment of 0.1 for BBOA in Qingdao yields 11 possible solutions, and for both HOA and CCOA in Dongguan yields 121 possible solutions.

4. Criteria for obtaining the optimal results.

In this study, we used two simple and reasonable criteria to obtain a better environmental OA source apportionment: the reasonability of the O/C ratio and the correlation between the factors and the tracers. For Qingdao, the O/C ratios for six resolved factors and the correlations between CCOA and PAHs, HOA and BC for 11 solutions with different  $a$  values are shown in Table S2. These results indicate that all of the O/C ratios for each factor and each factor-tracer correlation are quite similar to one another and that they agree with the range of values in the literature (Canagaratna et al., 2015). Therefore, the solutions averaged over the 11 outputs were considered the final results for Qingdao. For Dongguan, all of the O/C ratios for HOA, CCOA, COA and BBOA among the 121 possible solutions are listed in Table S3. The O/C ratio of HOA in the unconstrained PMF results remained between approximately 0.17 and 0.18, providing a filter criterion with which to assess reasonable ME-2 solutions, and only solutions with  $a$  values between 0 and 0.1 fell into this range (Table S1). The O/C ratios of other factors for  $a$  values between 0 and 0.1 are shown in Table S3. The solutions using  $a$  values between 0 and 0.1 for the HOA profile and an  $a$  value of 0.9 for the CCOA profile are considered ideal results for three reasons. First, unlike the HOA mass spectra, CCOAs from different sites show higher variability and the CCOA anchor profile is not derived from itself, and therefore, it is reasonable to restrict the constraint with small  $a$  values for HOA and a looser constraint should be applied for CCOA, which is consistent with the  $a$  values selecting rules in London ME-2 study (Reyes-Villegas et al., 2016). Second, the

186 POA factors in Dongguan, including HOA and CCOA, have higher O/C ratios likely as a result of a higher atmospheric  
187 oxidizing capacity and a stronger photochemical formation in Southern China (Hofzumahaus et al., 2009). Moreover, some  
188 studies reported that BBOAs undergo substantial chemical processing immediately after emission and that aged BBOAs had  
189 significant concentrations in fresh plumes (Zhou et al., 2017). Thus, CCOAs in Dongguan are very likely to demonstrate  
190 relatively higher ages than those in Qingdao (0.15) with higher O/C ratios (but with an O/C ratio of up to 1.25 when the  $\alpha$   
191 value is 1, which is unacceptable). Third, with an increase in the  $\alpha$  value for CCOA, two types of OOA become more  
192 distinctive, and the factor correlates better with the tracer (Table S1 and Table S4).

193 In order to prove the improvement of using the anchor profiles generated by the unconstrained PMF run with the same  
194 local datasets, we also run the ME-2 analysis using the anchor profiles available in the literature, with the results shown in  
195 Table S5 and S6. For Qingdao, the correlations between POAs and their tracers and the Q/Q<sub>exp</sub> values using the three BBOA  
196 profiles in the literature are poorer than using the BBOA obtained in this study (Table S5). For Dongguan, the results from  
197 ME-2 using the HOA profiles in the literature are also poorer than using the HOA profiles obtained in this study (Table S6).  
198 Therefore, it can be clearly seen that the method to obtain an anchor profile in this study is easier (it does not depend on the  
199 results in the literature) and more valid.

## 200 4 Results and discussion

201

### 202 4.1 Variations in the OA factors

203 Figure 1 shows the chemical compounds of PM<sub>1</sub>, including the non-refractory (NR) components measured via HR-AMS  
204 (i.e., OA, SO<sub>4</sub>, NO<sub>3</sub>, NH<sub>4</sub> and Cl) and BC concentrations measured via the AE-31, during the sampling period in both Qingdao  
205 and Dongguan. The average PM<sub>1</sub> mass concentration was 32.1±21.2 μg/m<sup>3</sup> (mean ± standard deviation) in Qingdao and  
206 57.4±31.1 μg/m<sup>3</sup> in Dongguan. The temporal variations in the PM<sub>1</sub> species in conjunction with meteorological parameters are  
207 shown in Figure S5. Although Dongguan is located in southern China with relatively less air pollution (Huang et al., 2012),  
208 the PM<sub>1</sub> mass concentration was higher. This is mainly because of stagnant meteorological conditions with low average wind  
209 speeds (i.e., 2.3 m/s) and a maximum wind speed of less than 6 m/s. Among the PM<sub>1</sub> compounds, OAs accounted for 32.5%  
210 of PM<sub>1</sub> in Qingdao and 40.6% in Dongguan. This suggests that OA constitutes a very important fraction at both urban sites.  
211 Thus, the final and detailed results of the OA source apportionment are presented in this section.

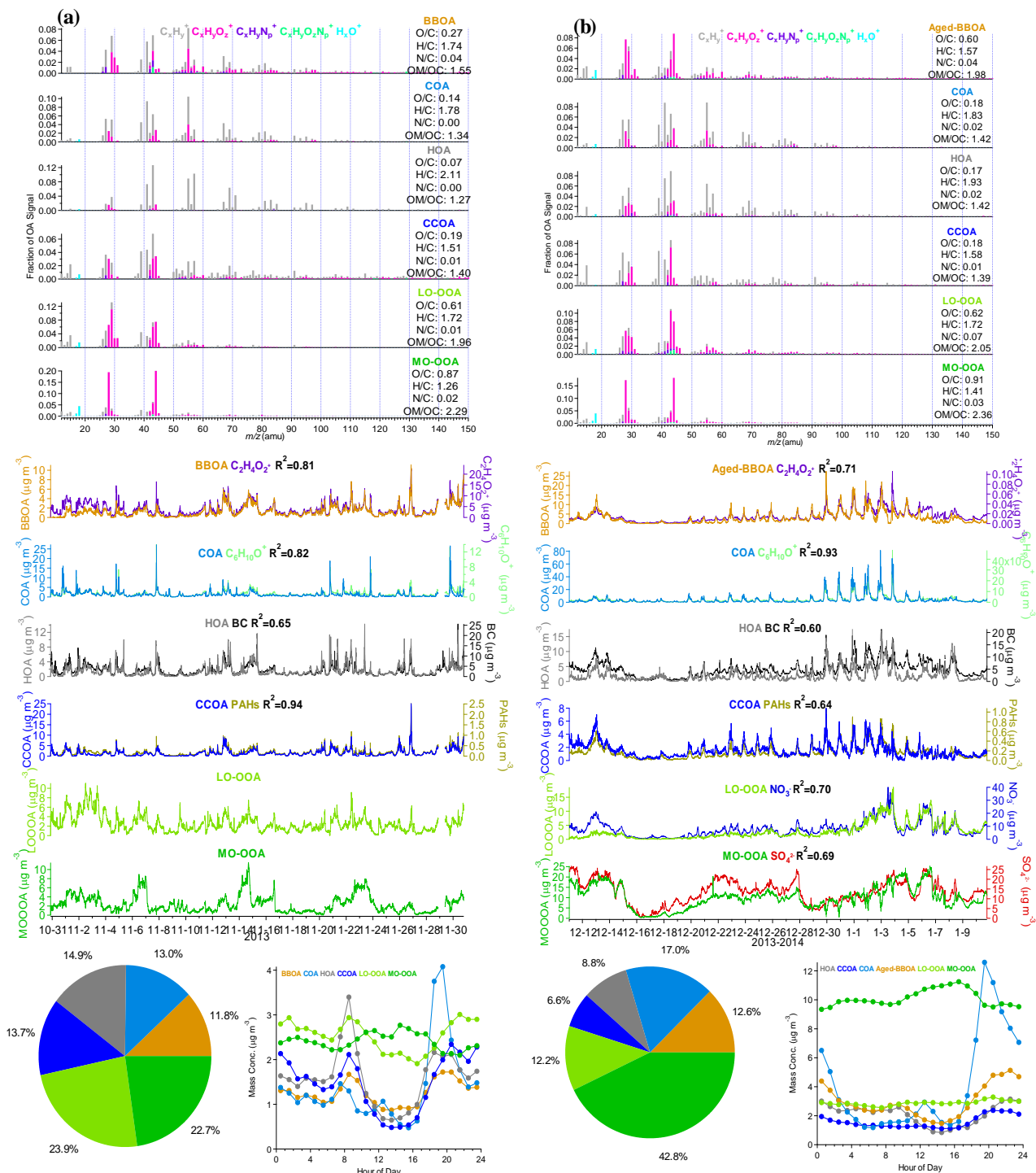
212 For Qingdao, the final result is the average of all of the ME-2 runs with constraints including  $\alpha$  values from 0 to 1 fulfilling  
213 the criteria described in section 3.2. The mass spectra and time series of the resolved OA sources are shown in Figure 3a. The  
214 characteristics of each factor were distinct. The BBOA profile contained the highest  $m/z$  60 fraction  $f_{60}$  (1.5%) compared to  
215 the other factors, and the concentrations were highly correlated with C<sub>2</sub>H<sub>4</sub>O<sub>2</sub><sup>+</sup> (R<sup>2</sup>=0.81). The mass spectra of COA was  
216 characterized by a high  $m/z$  55/57 ratio, which is consistent with previous results (He et al., 2010; Mohr et al., 2012; Sun et al.,

217 2016). In addition, the time series of COA showed a good correlation with its tracer ion  $C_6H_{10}O^+$  in accordance with (Sun et  
218 al., 2016). HOAs were correlated well with BC ( $R^2=0.65$ ), and CCOAs were highly correlated with PAHs ( $R^2=0.94$ ). Among  
219 the two types of OOAs, the less-oxidized OOA (LO-OOA) had a lower  $CO_2^+$  fraction and O/C ratio (0.62) compared with the  
220 more oxidized OOA (MO-OOA), which had a higher  $CO_2^+$  fraction and O/C (0.91) ratio. The sum of LO-OOA and MO-OOA  
221 showed a high correlation with the sum of sulfate and nitrate ( $R^2=0.76$ ). The POAs (including HOA, COA, BBOA and CCOA)  
222 contributed 53.4% to the OA concentration (Figure 3a), which was almost equal to the SOA fraction. In terms of the diurnal  
223 trends of the OA factors shown in Figure 3a, they are all partially driven both by PBL dynamics (demonstrating an increased  
224 dilution during the daytime and an accumulation of particulate matter overnight) and by the diurnal emission profile. The  
225 diurnal trend of HOA showed pronounced peaks during the morning and evening rush hours (8:00-9:00 and 19:00-21:00),  
226 which is typically the case for traffic-related pollutants. COA shows a very distinct daily trend with strong peaks during the  
227 lunch (approximately 12:00) and dinner (19:00-20:00) periods. CCOAs constituted an important and dominant source of  
228 pollutants during the wintertime in northern Chinese areas (Elser et al., 2016) due to heating activities, especially with regard  
229 to the central-heating supply that began on November 13 and continued until the end of the campaign. The diurnal variations  
230 of the four POA factors before and during the central-heating period are shown in Figure S6. In comparison with the other  
231 three POAs, the diurnal pattern of CCOA showed a clear increase during the central-heating period with concentration peaks  
232 during the morning (at approximately 9:00) and at night (starting to rise at 18:00), which seems consistent with heating  
233 emissions and atmospheric dilution. The diurnal trends of BBOA were similar to those of CCOA. The dilution of these particles  
234 within a deeper PBL during the daytime resulted in a decreasing trend in the BBOA concentration, while peaks related to  
235 residential heating were observed during the morning (between 09:00 to 10:00) and at night (starting to rise at 17:00). The  
236 main difference between the LO-OOA and MO-OOA diurnal patterns is that an increase in the MO-OOA mass concentration  
237 was observed during the daytime, implying that the formation of secondary organic aerosols was greatly enhanced during the  
238 afternoon. In addition, the diurnal cycle for LO-OOA showed a relatively smaller decrease during the daytime compared with  
239 the POA factors. These characteristics of the OOA diurnal trend confirm their secondary nature.

240 For Dongguan, similar to the OA source apportionment using ME-2 in Qingdao, the final result is the average of two  
241 accepted a-value solutions with six identified factors, including HOA, CCOA, COA, Aged-BBOA, LO-OOA and MO-OOA.  
242 Although the range of the O/C ratio of BBOA reported in Canagaratna et al. (2015) was from 0.25 to 0.55, fresh BBOA was  
243 found to be rapidly converted to OOA in less than 1 day (Bougiatioti et al., 2014), and the O/C ratio of aged BBOA could be  
244 up to 0.85 (Zheng et al., 2017). BBOA in Dongguan was apparently not fresh considering it is an urban site and Dongguan has  
245 a warmer winter (17 °C in Dongguan vs. 9 °C in Qingdao). The BBOA factor identified in Dongguan, with a strong contribution  
246 of m/z 60, had a higher O/C, indicating it was an oxygenated BBOA, therefore we name it Aged-BBOA in this study. All of  
247 the information regarding the final source results is shown in Figure 3b. Good correlations between each OA factor and their  
248 tracers indicate that the resolved ME-2 results are reasonable. A few sharp drops (which always occurred at approximately  
249 20:00) were observed in the MO-OOA time series ranging from December 29 to January 5, which coincides with extreme  
250 organic aerosol pollution (Figure S5). The inherent mechanisms for these drops remain unexplained, although we have tried a

251 number of reasonable approaches (e.g., splitting the period into sub-periods to identify the sources, constraining more factors  
252 before running ME-2, and examining more factors) to address this issue. A similar problem in the MO-OOA time series was  
253 also found in a recent ME-2 application (Qin et al., 2017). In our case, we presume this might be the result of relatively worse  
254 meteorological conditions at night during the sampling period, thereby increasing the contribution of late supper emissions  
255 and leading to the overestimation of COAs offset by drops in the MO-OOA concentration. Also note that the O/C ratios of the  
256 POAs in Dongguan were higher than those in Qingdao, suggesting that POA emissions in Dongguan underwent faster chemical  
257 processing. In addition, the relatively smaller contributions of POAs further support this inference. Freshly emitted POAs may  
258 get mixed with aged OAs more easily, while ME-2 may still consider them unmixed. MO-OOAs accounted for an average of  
259 42.8% of the total OA mass (which is much greater than the contribution of LO-OOAs), which is probably because some POA  
260 species could have been rapidly converted to very aged OOs (Bougiatioti et al., 2014; Xu et al., 2015). As mentioned above,  
261 the characteristics of the diurnal trends of the POA factors in Dongguan were similar to those in Qingdao, and thus, we focused  
262 on the OOA factors. MO-OOAs still showed higher concentrations during the daytime but, unlike LO-OOAs in Qingdao, the  
263 diurnal patterns of LO-OOAs in Dongguan were flat, implying that secondary OA formation in the LO-OOAs basically offset  
264 the influences of PBL variations.

265 Meteorological conditions (especially wind) play a crucial role in the dilution and transport of air pollution. We used the  
266 relationships between the component concentrations and wind to profoundly understand the origins of the OA factors and their  
267 nature. The distributions of the OA factor concentrations versus the wind direction and speed are plotted in Figure S7. For  
268 both of the urban sites, higher mass concentrations of the POA factors were mostly accompanied by low wind speeds, denoting  
269 their local emission characteristics. Additionally, for the OOA factors, a large proportion of their higher concentrations were  
270 maintained at higher wind speeds, indicating that the OOs were formed by transport processes. However, the small fraction  
271 of high-level OOs that was concentrated within the low wind-speed region represents the fast formation of OOs from some  
272 local POA.



273  
 274 **Figure 3.** Mass spectra of the OA factors, average fractions of the OA factors, diurnal variations of the OA factors and time  
 275 series of the OA factors identified by the ME-2 method for (a)Qingdao and (b) Dongguan.

## 4.2 Regression analysis for POA tracers

278 BC and PAHs are mainly derived from incomplete combustion processes (Schmidt and Noack, 2000; White, 1985), and  
279 thus, they were used as tracers for the POAs. In this study, the BC was directly measured by the AE-31, and the PAHs were  
280 quantified using the method developed by Bruns et al. (2015) based on AMS data. Both the BC and PAHs showed pronounced  
281 diurnal cycles similar to those of the POAs (see Figure S8). In addition, POAs are properly split into different subtypes via the  
282 ME-2 method, thereby providing the possibility to better understand the contributions of different POAs to BC and PAHs and  
283 to verify the POA source identification. In this section, we use a multi-linear regression method to analyze the POA factors for  
284 BC and PAHs.

285 Figure 4 shows the average contributions of OA sources to BC and PAHs in Qingdao and Dongguan. At both sites, HOAs  
286 were the dominant attribute of BC (51% for Qingdao and 40% for Dongguan) and CCOAs contributed the most to the PAHs  
287 (59% for Qingdao and 43% for Dongguan), indicating that BC mainly originates from traffic emissions and that PAHs in the  
288 Chinese urban polluted atmosphere are dominated by coal combustion during the wintertime. These findings are consistent  
289 with results reported in similar studies (Elser et al., 2016; Huang et al., 2015; Huang et al., 2010; Sun et al., 2016; Xu et al.,  
290 2014; Zhang et al., 2008). Moreover, the ratio of PAHs to OAs (1.8%) in Qingdao was similar to that in the northern Chinese  
291 urban site of Xi'an (1.9%) (Elser et al., 2016) but was higher than that in Dongguan (0.9%). This is likely because a larger  
292 fraction of coal combustion to the total OA concentration would enhance the ratio of PAHs to OAs (Elser et al., 2016). Biomass  
293 burning was the second-most important source for both BC and PAHs; it was responsible for 33% and 29% of the BC at  
294 Qingdao and Dongguan, respectively, and for 29% and 34% of the PAHs at Qingdao and Dongguan, respectively. Cooking  
295 emissions were a minor source of BC and PAHs, accounting for less than 10%. These results are also consistent with the  
296 published findings. For example, biomass burning is an important source for BC (Kondo et al., 2011; Reddy et al., 2002) and,  
297 in some regions with fewer traffic emissions, BC has the best correlation with BBOAs (Schwarz et al., 2008). In addition, in  
298 Beijing and California, PAHs are correlated well with BBOAs but are much more weakly correlated with COAs (Ge et al.,  
299 2012; Hu et al., 2016; Sun et al., 2016).

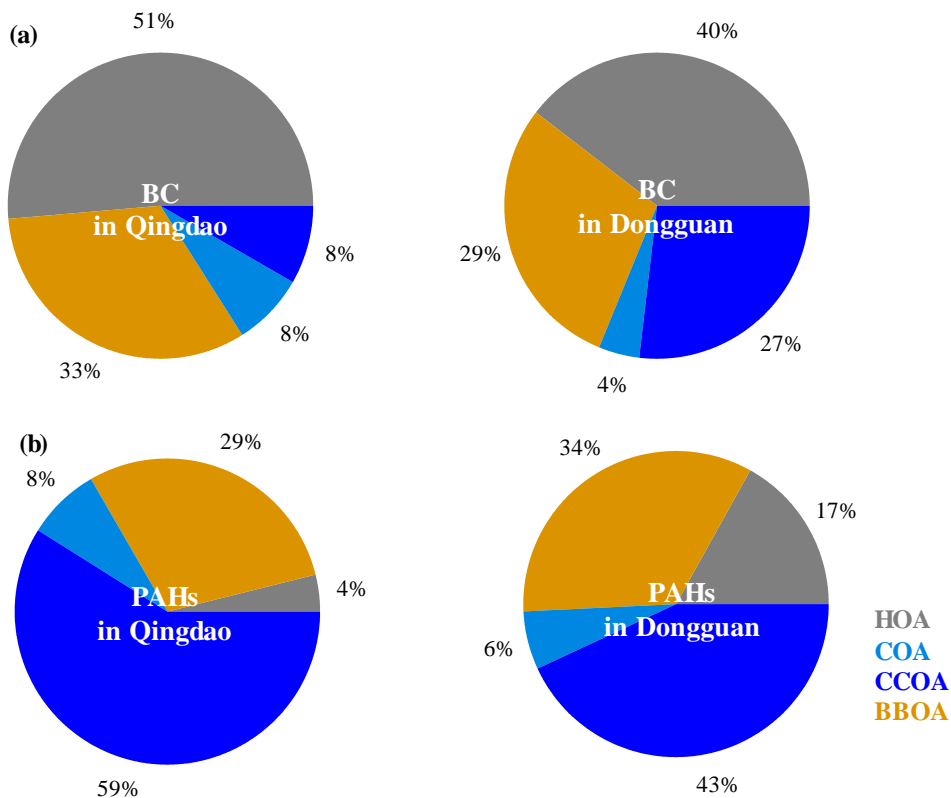


**Figure 4.** (a) Average contributions of POA factors to BC; (b) average contributions of POA factors to PAHs.

## 5 Conclusions

In this study, we used PMF to interpret the organic aerosol sources at two Chinese urban sites in winter, and found that PMF did not work properly (i.e., it did not allow for the separation of several primary sources of OAs). Therefore, we adopted the ME-2 approach, which yields more reliable solutions. Technically, there are three important steps when using the ME-2 method to interpret the sources of OAs. The first step is to investigate the mixed and unidentified factors that are constrained according to issues in the unconstrained PMF results. Generally, we constrained one or more POA factors (i.e., HOA, COA, BBOA and CCOA) for the polluted urban sites. The second step is to search for a reasonable anchor profile for each constrained factor. Two approaches were used: searching for anchor profiles via an increase in the number of unconstrained PMF factors from the same data set and using mass profiles derived from other similar studies. The third step is to choose the criteria for obtaining the optimal results. The choice of a reasonable range of O/C ratios may represent a good criterion for HR-OA apportionment since the O/C ratio is a significant and distinctive characteristic for different OA factors. In addition, correlations between the resolved OA factors and their tracers were also suggested.



314 **Acknowledgments**

315 This work was supported by the National Natural Science Foundation of China (91744202, U1301234), the Ministry of  
316 Science and Technology of China (2017YFC0210004), and the Science and Technology Plan of Shenzhen Municipality  
317 (JCYJ20170412150626172).

318 **References**

- 319 Aiken, A. C., D. Salcedo, M. J. Cubison, J. A. Huffman, P. F. DeCarlo, I. M. Ulbrich, K. S. Docherty, D. Sueper, J. R.  
320 Kimmel, D. R. Worsnop, A. Trimborn, M. Northway, E. A. Stone, J. J. Schauer, R. M. Volkamer, E. Fortner, B. de Foy,  
321 J. Wang, A. Laskin, V. Shutthanandan, J. Zheng, R. Zhang, J. Gaffney, N. A. Marley, G. Paredes-Miranda, W. P. Arnott,  
322 L. T. Molina, G. Sosa, and J. L. Jimenez : Mexico City aerosol analysis during MILAGRO using high resolution aerosol  
323 mass spectrometry at the urban supersite (T0) – Part 1: Fine particle composition and organic source apportionment,  
324 *Atmos. Chem. Phys.*, 9(17), 6633-6653, doi: 10.5194/acp-9-6633-2009,2009.
- 325 Alfarra, M. R., A. S. H. Prevot, S. Szidat, J. Sandradewi, S. Weimer, V. A. Lanz, D. Schreiber, M. Mohr, and U.  
326 Baltensperger : Identification of the Mass Spectral Signature of Organic Aerosols from Wood Burning Emissions,  
327 *Environ Sci. Technol.*, 41(16), 5770-5777, doi: 10.1021/es062289b,2007.
- 328 Allan, J. D., A. E. Delia, H. Coe, K. N. Bower, M. R. Alfarra, J. L. Jimenez, A. M. Middlebrook, F. Drewnick, T. B. Onasch,  
329 M. R. Canagaratna, J. T. Jayne, and D. R. Worsnop: A generalised method for the extraction of chemically resolved mass  
330 spectra from Aerodyne aerosol mass spectrometer data, *J. Aerosol Sci.*, 35(7), 909-922, doi:  
331 <https://doi.org/10.1016/j.jaerosci.2004.02.007>,2004.
- 332 Bougiatioti, A., I. Stavroulas, E. Kostenidou, P. Zarnmpas, C. Theodosi, G. Kouvarakis, F. Canonaco, A. S. H. Prévôt, A.  
333 Nenes, S. N. Pandis, and N. Mihalopoulos : Processing of biomass-burning aerosol in the eastern Mediterranean during  
334 summertime, *Atmos. Chem. Phys.*, 14(9), 4793-4807, doi: 10.5194/acp-14-4793-2014,2014.
- 335 Bruns, E. A., M. Krapf, J. Orasche, Y. Huang, R. Zimmermann, L. Drinovec, G. Močnik, I. El-Haddad, J. G. Slowik, J.  
336 Dommen, U. Baltensperger, and A. S. H. Prévôt : Characterization of primary and secondary wood combustion products  
337 generated under different burner loads, *Atmos. Chem. Phys.*, 15(5), 2825-2841, doi: 10.5194/acp-15-2825-2015,2015.
- 338 Canagaratna, M. R., J. L. Jimenez, J. H. Kroll, Q. Chen, S. H. Kessler, P. Massoli, L. Hildebrandt Ruiz, E. Fortner, L. R.  
339 Williams, K. R. Wilson, J. D. Surratt, N. M. Donahue, J. T. Jayne, and D. R. Worsnop : Elemental ratio measurements of  
340 organic compounds using aerosol mass spectrometry: characterization, improved calibration, and implications, *Atmos.*  
341 *Chem. Phys.*, 15(1), 253-272, doi: 10.5194/acp-15-253-2015,2015.
- 342 Canagaratna, M. R., J. T. Jayne, J. L. Jimenez, J. D. Allan, M. R. Alfarra, Q. Zhang, T. B. Onasch, F. Drewnick, H. Coe, A.  
343 Middlebrook, A. Delia, L. R. Williams, A. M. Trimborn, M. J. Northway, P. F. DeCarlo, C. E. Kolb, P. Davidovits, and

344 D. R. Worsnop : Chemical and microphysical characterization of ambient aerosols with the aerodyne aerosol mass  
345 spectrometer, *Mass Spectrom. Rev.*, 26(2), 185-222, doi: 10.1002/mas.20115,2007.

346 Canonaco, F., M. Crippa, J. G. Slowik, U. Baltensperger, and A. S. H. Prévôt : SoFi, an IGOR-based interface for the  
347 efficient use of the generalized multilinear engine (ME-2) for the source apportionment: ME-2 application to aerosol  
348 mass spectrometer data, *Atmos. Meas. Tech.*, 6(12), 3649-3661, doi: 10.5194/amt-6-3649-2013,2013.

349 Crippa, M., DeCarlo, P. F., Slowik, J. G., Mohr, C., Heringa, M.F., Chirico, R., Poulain, L., Freutel, F., Sciare, J., Cozic, J.,  
350 DiMarco, C. F., Elsasser, M., José, N., Marchand, N., Abidi, E., Wiedensohler, A., Drewnick, F., Schneider, J.,  
351 Borrmann, S., Nemitz, E., Zimmermann, R., Jaffrezo, J.-L., Prévôt, A. S. H., and Baltensperger, U.: Wintertime aerosol  
352 chemical composition and source apportionment of the organic fraction in the metropolitan area of Paris, *Atmos. Chem.  
353 Phys.*, 13, 961–981, doi:10.5194/acp-13-961-2013, 2013.

354 Crippa, M., F. Canonaco, V. a. Lanz, M. Äijälä, J. D. Allan, S. Carbone, G. Capes, D. Ceburnis, M. Dall'Osto, D. A. Day, P.  
355 F. DeCarlo, M. Ehn, a. Eriksson, E. Freney, L. Hildebrandt Ruiz, R. Hillamo, J. L. Jimenez, H. Junninen, A. Kiendler-  
356 Scharr, A. M. Kortelainen, M. Kulmala, A. Laaksonen, A. A. Mensah, C. Mohr, E. Nemitz, C. O'Dowd, J. Ovadnevaite,  
357 S. N. Pandis, T. Petäjä, L. Poulain, S. Saarikoski, K. Sellegri, E. Swietlicki, P. Tiitta, D. R. Worsnop, U. Baltensperger,  
358 and A. S. H. Prévôt: Organic aerosol components derived from 25 AMS data sets across Europe using a consistent ME-2  
359 based source apportionment approach, *Atmos. Chem. Phys.*, 14(12), 6159-6176, doi: 10.5194/acp-14-6159-2014, 2014.

360 Docherty, K. S., E. A. Stone, I. M. Ulbrich, P. F. DeCarlo, D. C. Snyder, J. J. Schauer, R. E. Peltier, R. J. Weber, S. M.  
361 Murphy, J. H. Seinfeld, B. D. Grover, D. J. Eatough, and J. L. Jimenez : Apportionment of Primary and Secondary  
362 Organic Aerosols in Southern California during the 2005 Study of Organic Aerosols in Riverside (SOAR-1), *Environ  
363 Sci. Technol.*, 42(20), 7655-7662, doi: 10.1021/es8008166,2008.

364 Drewnick, F., S. S. Hings, P. DeCarlo, J. T. Jayne, M. Gonin, K. Fuhrer, S. Weimer, J. L. Jimenez, K. L. Demerjian, S.  
365 Borrmann, and D. R. Worsnop : A New Time-of-Flight Aerosol Mass Spectrometer (TOF-AMS)—Instrument  
366 Description and First Field Deployment, *Aerosol Sci. Tech.*, 39(7), 637-658, doi: 10.1080/02786820500182040,2005.

367 Elser, M., R. J. Huang, R. Wolf, J. G. Slowik, Q. Wang, F. Canonaco, G. Li, C. Bozzetti, K. R. Daellenbach, Y. Huang, R.  
368 Zhang, Z. Li, J. Cao, U. Baltensperger, I. El-Haddad, and A. S. H. Prévôt : New insights into PM<sub>2.5</sub> chemical  
369 composition and sources in two major cities in China during extreme haze events using aerosol mass spectrometry,  
370 *Atmos. Chem. Phys.*, 16(5), 3207-3225, doi: 10.5194/acp-16-3207-2016,2016.

371 Fröhlich, R., V. Crenn, A. Setyan, C. A. Belis, F. Canonaco, O. Favez, V. Riffault, J. G. Slowik, W. Aas, M. Äijälä, A.  
372 Alastuey, B. Artiñano, N. Bonnaire, C. Bozzetti, M. Bressi, C. Carbone, E. Coz, P. L. Croteau, M. J. Cubison, J. K.  
373 Esser-Gietl, D. C. Green, V. Gros, L. Heikkinen, H. Herrmann, J. T. Jayne, C. R. Lunder, M. C. Minguillón, G. Močnik,  
374 C. D. O'Dowd, J. Ovadnevaite, E. Petralia, L. Poulain, M. Priestman, A. Ripoll, R. Sarda-Estève, A. Wiedensohler, U.  
375 Baltensperger, J. Sciare, and A. S. H. Prévôt : ACTRIS ACSM intercomparison – Part 2: Intercomparison of ME-2  
376 organic source apportionment results from 15 individual, co-located aerosol mass spectrometers, *Atmos. Meas. Tech.*,  
377 8(6), 2555-2576, doi: 10.5194/amt-8-2555-2015,2015.

378 Ge, X., A. Setyan, Y. Sun, and Q. Zhang : Primary and secondary organic aerosols in Fresno, California during wintertime:  
379 Results from high resolution aerosol mass spectrometry, *J. Geophys. Res.-Atmos.*, 117(D19), 161-169, doi:  
380 10.1029/2012JD018026,2012.

381 Hallquist, M., J. C. Wenger, U. Baltensperger, Y. Rudich, D. Simpson, M. Claeys, J. Dommen, N. M. Donahue, C. George,  
382 A. H. Goldstein, J. F. Hamilton, H. Herrmann, T. Hoffmann, Y. Iinuma, M. Jang, M. E. Jenkin, J. L. Jimenez, A.  
383 Kiendler-Scharr, W. Maenhaut, G. McFiggans, T. F. Mentel, A. Monod, A. S. H. Prévôt, J. H. Seinfeld, J. D. Surratt, R.  
384 Szmigielski, and J. Wildt : The formation, properties and impact of secondary organic aerosol: current and emerging  
385 issues, *Atmos. Chem. Phys.*, 9(14), 5155-5236, doi: 10.5194/acp-9-5155-2009,2009.

386 He, L. Y., Y. Lin, X. F. Huang, S. Guo, L. Xue, Q. Su, M. Hu, S. J. Luan, and Y. H. Zhang : Characterization of high-  
387 resolution aerosol mass spectra of primary organic aerosol emissions from Chinese cooking and biomass burning,  
388 *Atmos. Chem. Phys.*, 10(23), 11535-11543, doi: 10.5194/acp-10-11535-2010,2010.

389 Hofzumahaus, A., F. Rohrer, K. Lu, B. Bohn, T. Brauers, C.-C. Chang, H. Fuchs, F. Holland, K. Kita, Y. Kondo, X. Li, S.  
390 Lou, M. Shao, L. Zeng, A. Wahner, and Y. Zhang : Amplified Trace Gas Removal in the Troposphere, *Science*,  
391 324(5935), 1702, doi: 10.1126/science.1164566,2009.

392 Hu, W., M. Hu, W. Hu, J. L. Jimenez, B. Yuan, W. Chen, M. Wang, Y. Wu, C. Chen, Z. Wang, J. Peng, L. Zeng, and M.  
393 Shao : Chemical composition, sources, and aging process of submicron aerosols in Beijing: Contrast between summer  
394 and winter, *J. Geophys. Res.-Atmos.*, 121(4), 1955-1977, doi: 10.1002/2015JD024020,2016.

395 Hu, W. W., M. Hu, B. Yuan, J. L. Jimenez, Q. Tang, J. F. Peng, W. Hu, M. Shao, M. Wang, L. M. Zeng, Y. S. Wu, Z. H.  
396 Gong, X. F. Huang, and L. Y. He: Insights on organic aerosol aging and the influence of coal combustion at a regional  
397 receptor site of central eastern China, *Atmos. Chem. Phys.*, 13(19), 10095-10112, doi: 10.5194/acp-13-10095-2013,2013.

398 Huang, R. J., Y. Zhang, C. Bozzetti, K. F. Ho, J. J. Cao, Y. Han, K. R. Daellenbach, J. G. Slowik, S. M. Platt, F. Canonaco,  
399 P. Zotter, R. Wolf, S. M. Pieber, E. A. Brunts, M. Crippa, G. Ciarelli, A. Piazzalunga, M. Schwikowski, G. Abbaszade, J.  
400 Schnelle-Kreis, R. Zimmermann, Z. An, S. Szidat, U. Baltensperger, I. El Haddad, and A. S. H. Prévôt: High secondary  
401 aerosol contribution to particulate pollution during haze events in China, *Nature*, 514(7521), 218-222, doi:  
402 10.1038/nature13774,2015.

403 Huang, X. F., L. Y. He, L. Xue, T. L. Sun, L. W. Zeng, Z. H. Gong, M. Hu, and T. Zhu: Highly time-resolved chemical  
404 characterization of atmospheric fine particles during 2010 Shanghai World Expo, *Atmos. Chem. Phys.*, 12(11), 4897-  
405 4907, doi: 10.5194/acp-12-4897-2012,2012.

406 Huang, X. F., L. Y. He, M. Hu, M. R. Canagaratna, Y. Sun, Q. Zhang, T. Zhu, L. Xue, L. W. Zeng, X. G. Liu, Y. H. Zhang,  
407 J. T. Jayne, N. L. Ng, and D. R. Worsnop : Highly time-resolved chemical characterization of atmospheric submicron  
408 particles during 2008 Beijing Olympic Games using an Aerodyne High-Resolution Aerosol Mass Spectrometer, *Atmos.*  
409 *Chem. Phys.*, 10(18), 8933-8945, doi: 10.5194/acp-10-8933-2010,2010.

410 IPCC , Climate Change 2013: The Physical Science Basis. Contribution of Working Group I to the Fifth Assessment Report  
411 of the Intergovernmental Panel on Climate Change, 1535 pp., Cambridge University Press, Cambridge, United Kingdom  
412 and New York, NY, USA,2013.

413 Jayne, J. T., D. C. Leard, X. Zhang, P. Davidovits, K. A. Smith, C. E. Kolb, and D. R. Worsnop :Development of an Aerosol  
414 Mass Spectrometer for Size and Composition Analysis of Submicron Particles, *Aerosol Sci. Tech.*, 33(1-2), 49-70, doi:  
415 10.1080/027868200410840,2000.

416 Jimenez, J. L., M. R. Canagaratna, N. M. Donahue, A. S. H. Prevot, Q. Zhang, J. H. Kroll, P. F. DeCarlo, J. D. Allan, H.  
417 Coe, N. L. Ng, A. C. Aiken, K. S. Docherty, I. M. Ulbrich, A. P. Grieshop, A. L. Robinson, J. Duplissy, J. D. Smith, K.  
418 R. Wilson, V. A. Lanz, C. Hueglin, Y. L. Sun, J. Tian, A. Laaksonen, T. Raatikainen, J. Rautiainen, P. Vaattovaara, M.  
419 Ehn, M. Kulmala, J. M. Tomlinson, D. R. Collins, M. J. Cubison, J. Dunlea, J. A. Huffman, T. B. Onasch, M. R. Alfarra,  
420 P. I. Williams, K. Bower, Y. Kondo, J. Schneider, F. Drewnick, S. Borrmann, S. Weimer, K. Demerjian, D. Salcedo, L.  
421 Cottrell, R. Griffin, A. Takami, T. Miyoshi, S. Hatakeyama, A. Shimono, J. Y. Sun, Y. M. Zhang, K. Dzepina, J. R.  
422 Kimmel, D. Sueper, J. T. Jayne, S. C. Herndon, A. M. Trimborn, L. R. Williams, E. C. Wood, A. M. Middlebrook, C. E.  
423 Kolb, U. Baltensperger, and D. R. Worsnop : Evolution of Organic Aerosols in the Atmosphere, *Science*, 326(5959),  
424 1525-1529, doi: 10.1126/science.1180353,2009.

425 Kondo, Y., H. Matsui, N. Moteki, L. Sahu, N. Takegawa, M. Kajino, Y. Zhao, M. J. Cubison, J. L. Jimenez, S. Vay, G. S.  
426 Diskin, B. Anderson, A. Wisthaler, T. Mikoviny, H. E. Fuelberg, D. R. Blake, G. Huey, A. J. Weinheimer, D. J. Knapp,  
427 and W. H. Brune: Emissions of black carbon, organic, and inorganic aerosols from biomass burning in North America  
428 and Asia in 2008, *J. Geophys. Res.-Atmos.*, 116(D8), 353-366, doi: 10.1029/2010JD015152,2011.

429 Lanz, V. A., M. R. Alfarra, U. Baltensperger, B. Buchmann, C. Hueglin, and A. S. H. Prévôt : Source apportionment of  
430 submicron organic aerosols at an urban site by factor analytical modelling of aerosol mass spectra, *Atmos. Chem. Phys.*,  
431 7(6), 1503-1522, doi: 10.5194/acp-7-1503-2007,2007.

432 Lanz, V. A., A. S. H. Prévôt, M. R. Alfarra, S. Weimer, C. Mohr, P. F. DeCarlo, M. F. D. Gianini, C. Hueglin, J. Schneider,  
433 O. Favez, B. D'Anna, C. George, and U. Baltensperger: Characterization of aerosol chemical composition with aerosol  
434 mass spectrometry in Central Europe: an overview, *Atmos. Chem. Phys.*, 10(21), 10453-10471, doi: 10.5194/acp-10-  
435 10453-2010,2010.

436 Matthew, B. M., A. M. Middlebrook, and T. B. Onasch : Collection Efficiencies in an Aerodyne Aerosol Mass Spectrometer  
437 as a Function of Particle Phase for Laboratory Generated Aerosols, *Aerosol Sci. Tech.*, 42(11), 884-898, doi:  
438 10.1080/02786820802356797,2008.

439 Middlebrook, A. M., R. Bahreini, J. L. Jimenez, and M. R. Canagaratna : Evaluation of Composition-Dependent Collection  
440 Efficiencies for the Aerodyne Aerosol Mass Spectrometer using Field Data, *Aerosol Sci. Tech.*, 46(3), 258-271, doi:  
441 10.1080/02786826.2011.620041,2012.

442 Mohr, C., P. F. DeCarlo, M. F. Heringa, R. Chirico, J. G. Slowik, R. Richter, C. Reche, A. Alastuey, X. Querol, R. Seco, J.  
443 Peñuelas, J. L. Jiménez, M. Crippa, R. Zimmermann, U. Baltensperger, and A. S. H. Prévôt : Identification and

444 quantification of organic aerosol from cooking and other sources in Barcelona using aerosol mass spectrometer data,  
445 Atmos. Chem. Phys., 12(4), 1649-1665, doi: 10.5194/acp-12-1649-2012,2012.

446 Ng, N. L., M. R. Canagaratna, J. L. Jimenez, Q. Zhang, I. M. Ulbrich, and D. R. Worsnop : Real-Time Methods for  
447 Estimating Organic Component Mass Concentrations from Aerosol Mass Spectrometer Data, Environ. Sci. Technol.,  
448 45(3), 910-916, doi: 10.1021/es102951k,2011.

449 Paatero, P. :The Multilinear Engine: A Table-Driven, Least Squares Program for Solving Multilinear Problems, including  
450 the n-Way Parallel Factor Analysis Model, J. Comput. Graph. Stat., 8(4), 854-888, doi: 10.2307/1390831,1999.

451 Paatero, P., and U. Tapper : Positive matrix factorization: A non-negative factor model with optimal utilization of error  
452 estimates of data values, Environmetrics, 5(2), 111-126, doi: 10.1002/env.3170050203,1994.

453 Pope, C. A., and D. W. Dockery : Health Effects of Fine Particulate Air Pollution: Lines that Connect, J. Air Waste  
454 Manage., 56(6), 709-742, doi: 10.1080/10473289.2006.10464485,2006.

455 Pratt, K. A., and K. A. Prather : Mass spectrometry of atmospheric aerosols—Recent developments and applications. Part II:  
456 On-line mass spectrometry techniques, Mass Spectrom. Rev., 31(1), 17-48, doi: 10.1002/mas.20330,2012.

457 Qin, Y. M., H. B. Tan, Y. J. Li, M. I. Schurman, F. Li, F. Canonaco, A. S. H. Prévôt, and C. K. Chan : Impacts of traffic  
458 emissions on atmospheric particulate nitrate and organics at a downwind site on the periphery of Guangzhou, China,  
459 Atmos. Chem. Phys., 17(17), 10245-10258, doi: 10.5194/acp-17-10245-2017,2017.

460 Reddy, C. M., A. Pearson, L. Xu, A. P. McNichol, B. A. Benner, S. A. Wise, G. A. Klouda, L. A. Currie, and T. I.  
461 Eglinton :Radiocarbon as a Tool To Apportion the Sources of Polycyclic Aromatic Hydrocarbons and Black Carbon in  
462 Environmental Samples, Environ. Sci. Technol., 36(8), 1774-1782, doi: 10.1021/es011343f,2002.

463 Reyes-Villegas, E., D. C. Green, M. Priestman, F. Canonaco, H. Coe, A. S. H. Prévôt, and J. D. Allan : Organic aerosol  
464 source apportionment in London 2013 with ME-2: exploring the solution space with annual and seasonal analysis,  
465 Atmos. Chem. Phys., 16(24), 15545-15559, doi: 10.5194/acp-16-15545-2016,2016.

466 Schmidt, M. W. I., and A. G. Noack : Black carbon in soils and sediments: Analysis, distribution, implications, and current  
467 challenges, Global Biogeochem. Cy., 14(3), 777-793, doi: 10.1029/1999GB001208,2000.

468 Schwarz, J. P., R. S. Gao, J. R. Spackman, L. A. Watts, D. S. Thomson, D. W. Fahey, T. B. Ryerson, J. Peischl, J. S.  
469 Holloway, M. Trainer, G. J. Frost, T. Baynard, D. A. Lack, J. A. de Gouw, C. Warneke, and L. A. Del  
470 Negro :Measurement of the mixing state, mass, and optical size of individual black carbon particles in urban and biomass  
471 burning emissions, Geophys. Res. Lett., 35(13), L13810, doi: 10.1029/2008GL033968,2008.

472 Sun, Y., W. Du, P. Fu, Q. Wang, J. Li, X. Ge, Q. Zhang, C. Zhu, L. Ren, W. Xu, J. Zhao, T. Han, D. R. Worsnop, and Z.  
473 Wang : Primary and secondary aerosols in Beijing in winter: sources, variations and processes, Atmos. Chem. Phys.,  
474 16(13), 8309-8329, doi: 10.5194/acp-16-8309-2016,2016.

475 Tian, H., Cheng, K., Wang, Y., Zhao, D., Lu, L., Jia, W. and Hao, J.: Temporal and spatial variation characteristics of  
476 atmospheric emissions of Cd, Cr, and Pb from coal in China. Atmospheric Environment, 50: 157-163,doi:  
477 10.1016/j.atmosenv.2011.12.045,2012.

478 Ulbrich, I. M., M. R. Canagaratna, Q. Zhang, D. R. Worsnop, and J. L. Jimenez : Interpretation of organic components from  
479 Positive Matrix Factorization of aerosol mass spectrometric data, *Atmos. Chem. Phys.*, 9(9), 2891-2918, doi:  
480 10.5194/acp-9-2891-2009,2009.

481 Wang, X., B. J. Williams, X. Wang, Y. Tang, Y. Huang, L. Kong, X. Yang, and P. Biswas : Characterization of organic  
482 aerosol produced during pulverized coal combustion in a drop tube furnace, *Atmos. Chem. Phys.*, 13(21), 10919-10932,  
483 doi: 10.5194/acp-13-10919-2013,2013.

484 White, H. :Black carbon in the environment, J. Wiley,1985.

485 Xu, J., Q. Zhang, M. Chen, X. Ge, J. Ren, and D. Qin: Chemical composition, sources, and processes of urban aerosols  
486 during summertime in northwest China: insights from high-resolution aerosol mass spectrometry, *Atmos. Chem. Phys.*,  
487 14(23), 12593-12611, doi: 10.5194/acp-14-12593-2014,2014.

488 Xu, L., S. Suresh, H. Guo, R. J. Weber, and N. L. Ng : Aerosol characterization over the southeastern United States using  
489 high-resolution aerosol mass spectrometry: spatial and seasonal variation of aerosol composition and sources with a  
490 focus on organic nitrates, *Atmos. Chem. Phys.*, 15(13), 7307-7336, doi: 10.5194/acp-15-7307-2015,2015.

491 Zhang, Q., J. L. Jimenez, M. R. Canagaratna, I. M. Ulbrich, N. L. Ng, D. R. Worsnop, and Y. Sun : Understanding  
492 atmospheric organic aerosols via factor analysis of aerosol mass spectrometry: a review, *Anal. Bioanal. Chem.*, 401(10),  
493 3045-3067, doi: 10.1007/s00216-011-5355-y,2011.

494 Zhang, Q., J. L. Jimenez, M. R. Canagaratna, J. D. Allan, H. Coe, I. Ulbrich, M. R. Alfarra, A. Takami, A. M. Middlebrook,  
495 Y. L. Sun, K. Dzepina, E. Dunlea, K. Docherty, P. F. DeCarlo, D. Salcedo, T. Onasch, J. T. Jayne, T. Miyoshi, A.  
496 Shimono, S. Hatakeyama, N. Takegawa, Y. Kondo, J. Schneider, F. Drewnick, S. Borrmann, S. Weimer, K. Demerjian,  
497 P. Williams, K. Bower, R. Bahreini, L. Cottrell, R. J. Griffin, J. Rautiainen, J. Y. Sun, Y. M. Zhang, and D. R.  
498 Worsnop :Ubiquity and dominance of oxygenated species in organic aerosols in anthropogenically-influenced Northern  
499 Hemisphere midlatitudes, *Geophys. Res. Lett.*, 34(13), L13801, doi: 10.1029/2007GL029979,2007.

500 Zhang, Y., J. J. Schauer, Y. Zhang, L. Zeng, Y. Wei, Y. Liu, and M. Shao : Characteristics of Particulate Carbon Emissions  
501 from Real-World Chinese Coal Combustion, *Environ Sci. Technol.*, 42(14), 5068-5073, doi: 10.1021/es7022576,2008.

502 Zhou, S., S. Collier, D. A. Jaffe, N. L. Briggs, J. Hee, A. J. Sedlacek Iii, L. Kleinman, T. B. Onasch, and Q. Zhang :  
503 Regional influence of wildfires on aerosol chemistry in the western US and insights into atmospheric aging of biomass  
504 burning organic aerosol, *Atmos. Chem. Phys.*, 17(3), 2477-2493, doi: 10.5194/acp-17-2477-2017,2017.

505